공학박사 학위논문

Charge carrier transport control of Metal-Insulator-Oxide Semiconductor-Metal (MIOSM) Thin-film diode (TFD)

금속-절연체-산화물 반도체-금속 적층 구조 박막 다이오드의 전하 캐리어 이동 제어에 관한 연구

2021년 2월

서울대학교 융합과학기술대학원

융합과학부 나노융합전공

박 준 우

Charge carrier transport control of Metal-Insulator-Oxide Semiconductor-Metal (MIOSM) Thin-film diode (TFD)

지도교수 김 연 상

이 논문을 공학박사학위 논문으로 제출함.

2021년 1월

서울대학교 융합과학기술대학원
융합과학부 나노융합전공

박 준 우

박준우의 박사학위 논문을 인준함

2021 년 1 월

위 원 장 박 원 철 (인)

부위원장 김 연 상 (인)

위 원 이 강 원 (인)

위 원 김 정 민 (인)

위 원 유 지 영 (인)

Abstract

Charge carrier transport control of Metal-Insulator-Oxide Semiconductor-Metal (MIOSM) Thin-film diode (TFD)

Jun-Woo Park

Program in Nano Science and Technology

The Graduate School of Convergence Science & Technology

Seoul National University

Oxide thin-film diodes (TFDs) and thin-film transistors (TFTs), which act as switching elements, are essential elements for the next-generation circuits. However, unlike oxide TFTs that have been successfully debuted in the industry, developments related to oxide TFDs are relatively slow. Recently, a new type of metal-insulator-oxide semiconductor-metal (MIOSM) structure oxide TFD has been introduced, which overcomes the problems of the conventional oxide TFDs such as P-N diodes, MIM diodes, and Schottky diodes that show electrical instability, narrow voltage

operating range, and low rectification ratio. The new oxide TFD is based on a principle of which charge carriers move through trap states inside the insulator when the charges are injected from the oxide semiconductor surface, and carriers cannot be injected into the insulator when the oxide semiconductor surface is depleted. Using these characteristics, a new concept of a TFD has been developed recently with superior stability and a high rectification ratio in metal-insulator-oxide semiconductor-metal (MIOSM) structures. However, all of the previously announced MIOSM TFDs have been fabricated based on n-type oxide materials. The development of MIOSM TFDs with p-type oxide materials is required for the flexibility of the electronic circuit configuration. In addition, various types of MIOSM TFDs such as low-voltage driving, high-voltage response, and Zener diode are necessary to increase the scalability of new TFDs. On the other hands, finding a way to shift the diode's turn-on voltage for the various specifications and applications of MIOSM TFDs remains a challenge. All MIOSM TFDs reported so far have the characteristics of turning on at or near 0 V. MIOSM TFD requires further research on turn-on voltage control to broaden the various specifications and simplify the circuit design to be applied. Herein, I propose p-type nickel oxide-based MIOSM TFDs. Contrary to the conventional n-type oxide, the new p-type oxide diode rectifies current based on the hole conduction inside the insulator. Our new diodes show a stable

rectification ratio of over 10^5 and have the advantage of selectively narrowing or widening the operating voltage range from ±8 V to ±80 V. We also demonstrated the first transparent p-type MIOSM TFD by applying indium tin oxide (ITO) as an electrode. The new p-type nickel oxide-based TFDs, which can handle low voltage as well as high voltage, are expected to serve as a fundamental building block for next-generation electronic circuits along with n-type MIOSM TFDs. Most importantly, it is considered that various p-type oxide-based MIOSM TFDs will be developed based on this study. Meanwhile, I also propose a novel approach to shift the turn-on voltage of MIOSM TFDs. By adding a metal electrode to the oxide semiconductor, different shifts of the turn-on voltage of MIOSM TFDs could be realized depending on the characteristic variation of the Schottky contact between the metal electrode and the oxide semiconductor. These findings are expected to accelerate expanding diversity of MIOSM TFDs and facilitate the industrial application of MIOSM diodes.

Keywords: Thin-film diode (TFD), MIOSM TFD, P-type nickel oxide semiconductor, Schottky diode, Turn-on voltage shift, Transparent TFD

Student Number: 2017-36180

Contents

List of figures

oxide semiconductor-metal (MIOSM) thin-film diode (TFD), (b) the interface between SiO_2 and NiO_X, (c) the boundary between p^{++} Si and SiO_2, and (d) polycrystalline NiO_X film.

Figure 2.4. (a) Vertical current density-voltage (*J-V*) plot and fitting curves to verify space-charge-limited conduction (SCLC) in the SiO_2 layer with trap states. (b) Schematic of current flow inside the SiO_2 layer according to the hole accumulation and injecting at the NiO_X surface.

Figure 2.5. (a) Schematic figures illustrating carrier distribution inside the SiO_2 layer when the hole carriers are weakly injected from the p-type nickel oxide (NiO_X) to the trap states inside the SiO_2 layer. (b) Charge redistribution when the carrier transit time of weakly injected holes (τ_c) is longer than the dielectric relaxation time (τ_c). When the density of injected carrier (p_i) is smaller than the of thermally generated free carrier (p_0) in equilibrium, dielectric layer has a tendency to maintain the charge neutrality and it is called dielectric relaxation.

Figure 2.6. (a) Graphical schematic for the charge carrier behavior inside the SiO_2 layer when the carrier transit time of strongly injected holes (τ_c) is shorter than the dielectric relaxation time (τ_c). As strongly injected carriers fill the trap states inside the insulator, they exhibit traps-filled-

limited (TFL) behavior. (b) Very strongly injected carriers show trap-free behavior after filling all trap states inside the SiO_2 layer and follow Child's law.

Figure 2.7. (a) *J-V* relationship showing depletion and inversion of the NiO_X surface. (b) Schematic of blocking hole injection into the SiO_2 layer due to hole depletion of the NiO_X surface.

Figure 2.8. (a) *I-V* relationship showing that the operating voltage region of p-type NiO_X-based MIOSM TFD can be selectively adjusted according to SiO_2 thickness variation. (b) *I-V* relationship of p-type NiO_X-based MIOSM TFD showing stable driving in the high voltage range.

Figure 2.9. High-voltage withstand and electrical breakdown test for a MIOSM TFD based on p-type NiO_X with 100-nm thick SiO_2. The TFD showed a breakdown at -80 V when ±100 V was applied to the bottom electrode.

Figure 2.10. (a) Schematic figures illustrating the device structures and (b) *I-V* characteristics of the heavily boron-doped $Si/SiN_X/NiO_X/Au$ structure.

Figure 2.11. (a) Log-log relation between vertical current density and voltage characteristics for space-charge-limited conduction (SCLC) in the heavily boron-doped $Si/SiN_X/NiO_X/Au$ structure MIOSM TFD. The

charge transfer mechanism is divided into one part in which charge carriers injected from NiO_X surface into the trap states of the SiN_X layer move while filling the traps (Traps-filled-limit), and the other part which indicates the trap-free behavior when the carriers move without trapping (Child's law). (b) High-voltage withstand test for p-type NiO_X MIOSM TFD with 100-nm thick SiN_X. The TFD did not breakdown when biased from -100 V to 100 V.

Figure 2.12. (a) Schematic figures illustrating the device structures and (b) *I-V* characteristics of the transparent ITO/SiO_2/NiO_X/Au structure MIOSM TFD.

Figure 2.13. Log-log relation between vertical current density and voltage characteristics for space-charge-limited conduction (SCLC) in the transparent ITO/SiO_2/NiO_X/Au structure MIOSM TFD.

Chapter 3

Figure 3.1. (a) Schematic representation of the metal-insulator-oxide semiconductor-metal (MIOSM) device composed of sputtered electron injection layer (EIL), thermally grown electron transport layer (ETL) and electrodes. (b) Vertical current-voltage plots for the devices measured at

Figure 3.20. Vertical I-V relationships of IZO-based TFDs depending on the different ratio of indium to zinc ($I_{0.3}Z_{0.7}O$, $I_{0.5}Z_{0.5}O$, and $I_{0.7}Z_{0.3}O$) with Al and Ag electrode; On-current comparison of IZO/Al with different indium contents under positive bias (solid line); Comparison of IZO (7:3)/Ag and IZO (5:5)/Ag which maintains the off state and IZO (3:7)/Ag where the turn-on is present.

List of Publications

(1) **Park, J. W.**; Lee, D.; Cho, N. K.; Lee, J.; Kim, Y. S., Turn-On Voltage Shift of Metal-Insulator-Oxide Semiconductor Thin-Film Diode by Adding Schottky Diode in Reverse Direction. *ACS Appl. Electron Mater.* **2019,** *1* (4), 530-537.

(2) **Park, J. W.**‡; Lee, D.‡; Kim, K.; Cho, Y. H.; Kim, Y. S., Rectification Mechanism of a P-type Oxide-based Metal–Insulator–Oxide Semiconductor–Metal Thin-Film Diode. *ACS Appl. Electron Mater.* **2020,** *2* (12), 3946-3952.

(3) Kim, K.‡; **Park, J. W.**‡; Lee, D.; Cho, Y. H.; Kim, Y. S., Precise Turn-On Voltage Control of MIOSM Thin-Film Diodes with Amorphous Indium–Gallium–Zinc Oxide. *ACS Appl. Mater. Inter.* **2021,** *13* (1), 878-886.

(4) Lee, D.‡; **Park, J. W.**‡; Cho, N. K.; Lee, J.; Kim, Y. S., Verification of Charge Transfer in Metal-Insulator-Oxide Semiconductor Diodes via Defect Engineering of Insulator. *Sci. Rep.* **2019,** *9*, 10323.

(5) Lim, K. H.; Huh, J. E.; Lee, J.; Cho, N. K.; **Park, J. W.**; Nam, B. I.; Lee, E.; Kim, Y. S. Strong Influence of Humidity on Low-Temperature Thin-Film Fabrication via Metal Aqua Complex for High Performance Oxide

Semiconductor Thin-Film Transistors. *ACS Appl. Mater. Inter.* **2017,** *9* (1), 548-557.

(6) Nam, B. I.; Park, J. S.; Lim, K. H.; Ahn, Y. K.; Lee, J.; **Park, J. W.**; Cho, N. K.; Lee, D.; Lee, H. B. R.; Kim, Y. S. Conduction mechanism change with transport oxide layer thickness in oxide hetero-interface diode. *Appl. Phys. Lett.* **2017,** *111* (5), 053506.

(7) Lee, J.; Yoon, K.; Lim, K. H.; **Park, J. W.**; Lee, D.; Cho, N. K.; Kim, Y. S. Vertical Transport Control of Electrical Charge Carriers in Insulator/Oxide Semiconductor Hetero-structure. *Sci. Rep.* **2018,** *8*, 5643.

(8) Cho, N. K.; Park, J.; Lee, D.; **Park, J. W.**; Lee, W. H.; Kim, Y. S. Investigation of Vertical Current Phenomena in the Insulator/Oxide Semiconductor Heterojunction Using XPS Analysis and an Atmospheric-Pressure Plasma Treatment System. *ACS Appl. Electron Mater.* **2019,** *1* (8), 1698-1704.

(9) Lee, S. E.; Na, H. J.; Lee, E. G.; Park, J.; Kim, K.; Im, C.; **Park, J. W.**; Gong, Y. J.; Kim, Y. S. The effect of surface energy characterized functional groups of self-assembled monolayers for enhancing the electrical stability of oxide semiconductor thin film transistors. *Nanotechnology* **2020,** *31* (47), 475203.

Chapter 1 Introduction

1.1 Overview

The oxide thin-film diode (TFD) is required as a fundamental building block of the next-generation electronic circuit along with the oxide thin-film transistor (TFT).[1,2] However, compared to recent developments of oxide TFTs, the conventional oxide TFDs have limitations such as electrical instability, low rectification ratio, and narrow operating voltage range.[3-8] Recently, a new type of TFD has been introduced by combining the electrical properties of an n-type oxide semiconductor with the phenomenon that charge carriers can be injected into the insulator.[9-12] The new TFD with a metal-insulator-oxide semiconductor-metal (MIOSM) structure shows not only an excellent rectification ratio but also exhibits transparency. However, for the existing MIOSM TFD to have more diverse specifications, it had to break through several limitations. One of them is that it is necessary to manufacture MIOSM TFD based on p-type oxide, and the other is that it is essential to develop a diode with a controlled turn-on voltage. To guarantee the flexibility and scalability of the electronic circuit configuration, the development of p-type oxide-based MIOSM TFD, as well as turn-on voltage controlled, should be accomplished. Here, the p-type nickel oxide-based TFD is

reported. The p-type MIOSM TFD has a stable rectification ratio over 10^5, and the advantage of selectively narrowing or widening the operating voltage range from ±8 V to ±80 V. Moreover, the transparent p-type MIOSM TFD was demonstrated. A novel approach to shift the turn-on voltage of MIOS TFDs is also discussed. By adding a metal electrode to the oxide semiconductor, different shifts of the turn-on voltage of MIOS TFDs could be realized depending on the characteristic variation of the Schottky contact between the metal electrode and the oxide semiconductor. ZnO/Ag-based TFD shifted to 4.0 V due to the reverse Schottky diode formed on the oxide semiconductor. A-IGZO/Au-based TFD showed a turn-on voltage of 8.4 V. A-IGZO + AgO_X/Ag-based TFD turned on at 12.8 V due to the enhanced Schottky property. The new p-type oxide diode and turn-on voltage controlled MIOSM TFD, which can be manufactured by the various existing thin-film processes, are expected to contribute as an essential element of next-generation electronic circuits.

1.2 Conventional oxide thin-film diodes

Oxide is based on the various physical properties expressed at the interface, and numerous research topics related to this topic have been derived and dealt with in-depth in each field.[13] In particular, oxide materials have been applied to fields

such as organic solar cells and thin-film transistors and have consistently produced in-depth research results.[14] Diodes are also fundamental elements of electronic circuits such as transistors and have been applied to numerous electronic circuits. Therefore, various efforts have been made to fabricate oxide thin film diodes in multiple structural forms, such as a P-N junction diode, a metal-insulator-metal structured MIM diode, and a metal-oxide semiconductor structured MS diode. The oxide-based P-N junction diode was reported in 2003 by Hosono's group, famous for its research on oxide transistors.[3] However, compared to n-type oxide semiconductors, which have excellent electrical properties, the electrical properties of p-type oxide are relatively insufficient, so p-n junction thin-film diodes have had difficulties in manufacturing diodes that require low off-current and high rectification ratio. Thin-film diodes using oxides have also been studied in the form of metal-insulator-metal MIM diodes.[6] The MIM diode has a sandwich structure in which an oxide insulator is placed between the lower electrode and the upper electrode. An electric field is applied to both electrodes to pass the charge carriers by quantum tunneling, and the rectification effect is achieved by adjusting the height of the energy barrier between the electrode and the insulator. MIM diodes have been applied to various fields such as photodetectors, rectennas, and solar energy harvesting by applying

these characteristics. However, MIM diodes have also exhibited high off-current and low rectification ratio limitations due to thin insulators' physical limitations. The yield of large-area processes has also been an issue due to its thinness. Although graphene was applied to one of the electrodes to control the metal and the insulator's energy barrier effectively, there has been a limit to showing only a low rectification ratio of hundreds to thousands.[7] There have been attempts to fabricate a diode by depositing two insulators with different bandgaps in succession to achieve a high rectification ratio.[15] These cases also exhibited a low rectification ratio due to the material limitations of the thin insulator.

1.3 Conduction mechanisms in dielectric films

In the MIM diode, a tunneling-based conduction mechanism is used in which electric charges pass directly through the thin insulator. Mechanisms that describe the charge tunneling through the insulator include Schottky emission by thermal excitation, F-N tunneling through the energy barrier thinned by the applied field, and direct tunneling through the energy barrier (Figure 1.1. (a)).[16] This tunneling mechanism belongs to the electrode-limited transport mechanism that controls the tunneling charge's amount by controlling the energy barrier between the metal and the insulator.[17-20]

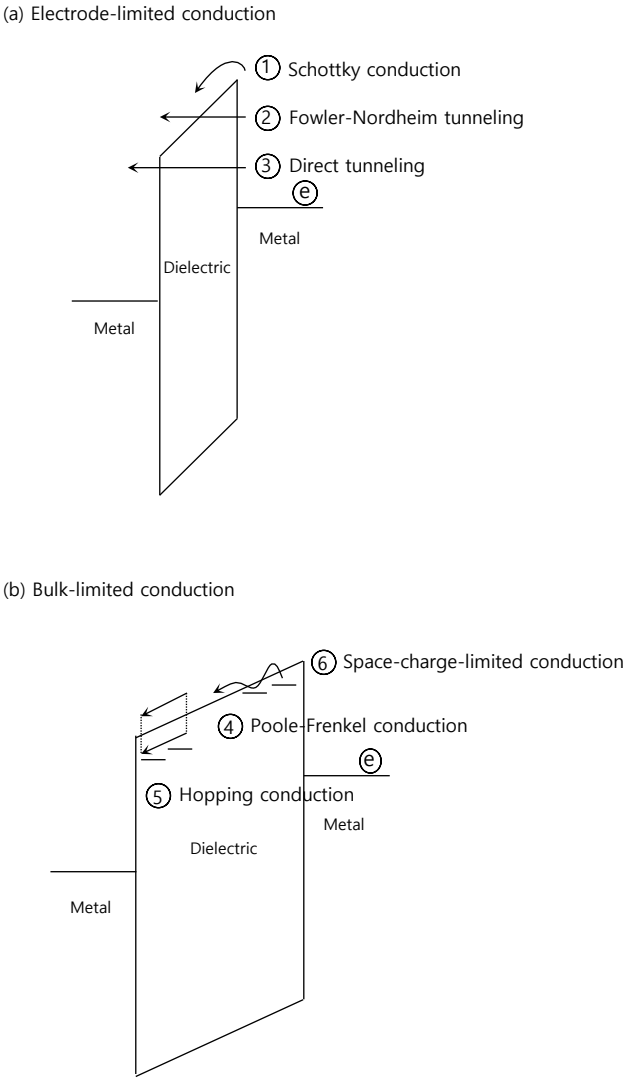

Figure 1.1. (a) Schematic diagram of the electrode-limited conduction mechanism in metal-insulator-metal (MIM) structure. (b) Schematic diagram of the bulk-limited conduction mechanism in MIM structure.[16]

On the other hand, naturally generated trap states always exist inside all insulators. When an electric field is applied at both ends of the insulator, charge carriers flow along with the trap states inside the insulator, and various charge transfer mechanisms that explain this phenomenon have been studied.[17-20] Mechanisms that explain the charge carriers' characteristics move along the insulator's trap states include Poole-Frenkel emission, Hopping conduction, and Ionic conduction (Figure 1.1. (b)). The trap states inside the insulator determine the charge transfer characteristic called a bulk-limited transport mechanism. Among these bulk-limited transport mechanisms, there is a space-charge-limited conduction (SCLC) mechanism. The SCLC mechanism is divided into one region that fills the trap states and the other region that all the traps are filled inside the insulator.

1.4 Metal-Insulator-Oxide Semiconductor-Metal (MIOSM) thin-film diode

Recently, a novel oxide thin-film diode using the SCLC mechanism has been reported.[9-12] This new diode exhibits a rectification ratio over 1000 times higher than that of conventional oxide-based TFDs. Figure 1.2. (a) shows the metal-insulator-metal (MIM) structure, and Figure 1.2. (b) shows the metal-insulator-

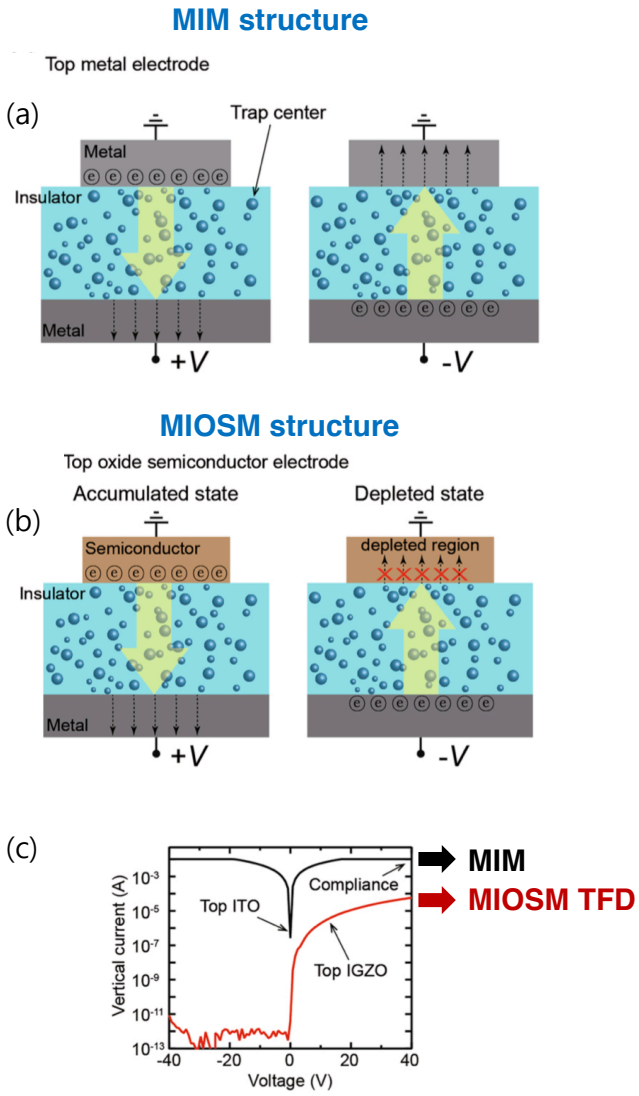

Figure 1.2. (a) Schematic diagram of the metal-insulator-metal (MIM) structure. (b) Schematic diagram of the metal-insulator-oxide semiconductor-metal (MIOSM) thin-film diode (TFD). (c) Vertical current-voltage characteristics of MIM and MIOSM devices.[10]

oxide semiconductor-metal (MIOSM) thin-film diode (TFD). The difference between Figure 1.2. (a) and (b) is whether the metal is used as the top electrode or a-IGZO is used as the top layer. However, the rectification characteristics of the two structures show different electrical characteristics. When metal is used for the top layer, current flows well in both directions regardless of the direction of the applied field, so that the rectification characteristic does not appear. However, MIOSM TFD shows a high rectification ratio over 10^6 when n-type a-IGZO is used as the top layer. When a positive bias is applied to the bottom electrode of MIOSM TFD, electrons are accumulated at the interface between the semiconductor and the insulator. The accumulated electrons are injected into trap states inside the insulator. As the voltage increases, the electric charges fill the trap states inside the insulator, and the current flows well in the vertical direction. However, when a negative bias is applied to the bottom electrode, n-type a-IGZO depletions at the interface with the insulator, preventing electrons from being injected into the insulator from the bottom electrode. As a result, vertical current does not flow inside the device, and the MIOSM structure device exhibits rectification characteristics. Each characteristic of the charge carrier's transfer depending on the accumulation/depletion of the oxide thin film (electrode-limited conduction mechanism) and the insulator material's trap states (bulk-limited

conduction mechanism) is the core operating principle of the MIOSM TFD. Based on this principle, the MIOSM TFD has advantages such as low off current, high on current, high asymmetry, and expandability in various operating voltage ranges, which conventional oxide TFDs have not achieved.

1.5 Motivation

Since the MIOSM TFD uses a single oxide semiconductor, the fabrication process is more straightforward than the P-N junction. It is also possible to fabricate a device with uniform electrical characteristics in a relatively large area than the MIM diode, which needs to control a thinner insulator thickness. In addition, when manufacturing MIOSM TFD, well-known semiconductor process equipment can be employed, and oxide insulators and semiconductors already widely used in the industry can be applied.

MIOSM TFD, which has such a number of advantages, has also had requirements to improve its deficiencies. MIOSM TFD with p-type oxide semiconductor and MIOSM TFD with adjustable turn-on voltage is indispensable in improving manufacturing convenience for circuits using new diodes and expanding diodes' applications.

All of the previously published papers for MIOSM TFDs have been

demonstrated based on n-type oxide semiconductors. However, for the flexibility of electronic circuit configuration, it is essential to fabricate MIOSM TFD using a p-type oxide semiconductor. Additionally, to secure new diodes of various specifications, diodes manufactured using p-type oxide semiconductors have to drive at low voltages, respond to high voltage operating, and need to have transparency as well.

Moreover, all MIOSM TFDs published so far must overcome the limitation of turning on the device near 0 V. A diode that turns on at a higher voltage, such as a Zener diode or a transient voltage suppression diode, must be developed in the form of an oxide thin film to diversify the specifications of the MIOSM TFD to increase the convenience of applying the device to a circuit.

1.6 Reference

(1) Fortunato, E.; Barquinha, P.; Martins, R., Oxide Semiconductor Thin-Film Transistors: A Review of Recent Advances. *Adv. Mater.* **2012,** *24* (22), 2945-2986.

(2) Shim, G. W.; Hong, W.; Cha, J. H.; Park, J. H.; Lee, K. J.; Choi, S. Y., TFT Channel Materials for Display Applications: From Amorphous Silicon to Transition Metal Dichalcogenides. *Adv. Mater.* **2020,** *32,* e1907166.

(3) Narushima, S.; Mizoguchi, H.; Shimizu, K.; Ueda, K.; Ohta, H.; Hirano, M.; Kamiya, T.; Hosono, H., A p-type amorphous oxide semiconductor and room temperature fabrication of amorphous oxide p-n heterojunction diodes. *Adv. Mater.* **2003,** *15* (17), 1409-1413.

(4) Cowell, E. W.; Alimardani, N.; Knutson, C. C.; Conley, J. F.; Keszler, D. A.; Gibbons, B. J.; Wager, J. F., Advancing MIM Electronics: Amorphous Metal Electrodes. *Adv. Mater.* **2011,** *23* (1), 74-78.

(5) Marques, G. C.; Tahoori, M.; Aghassi-Hagmann, J.; Sukuramsyah, A. M.; Rus, A. A.; Bolat, S.; Aribia, A.; Feng, X. W.; Singaraju, S. A.; Ramon, E.; Romanyuk, Y., Fabrication and Modeling of pn-Diodes Based on

Inkjet Printed Oxide Semiconductors. *IEEE Electr. Device L.* **2020,** *41* (1), 187-190.

(6) Periasamy, P.; Berry, J. J.; Dameron, A. A.; Bergeson, J. D.; Ginley, D. S.; O'Hayre, R. P.; Parilla, P. A., Fabrication and Characterization of MIM Diodes Based on Nb/Nb_2O_5 Via a Rapid Screening Technique. *Adv. Mater.* **2011,** *23* (27), 3080-3085.

(7) Urcuyo, R.; Duong, D. L.; Jeong, H. Y.; Burghard, M.; Kern, K., High Performance Graphene-Oxide-Metal Diode through Bias-Induced Barrier Height Modulation. *Adv. Electron Mater.* **2016,** *2* (9), 1600223.

(8) Son, Y.; Li, J. B.; Peterson, R. L., In Situ Chemical Modification of Schottky Barrier in Solution Processed Zinc Tin Oxide Diode. *ACS Appl. Mater. Inter.* **2016,** *8* (36), 23801-23809.

(9) Lee, E.; Lee, J.; Kim, J. H.; Lim, K. H.; Byun, J. S.; Ko, J.; Kim, Y. D.; Park, Y.; Kim, Y. S., Direct electron injection into an oxide insulator using a cathode buffer layer. *Nat. Commun.* **2015,** *6,* 1-6.

(10) Lee, J.; Yoon, K.; Lim, K. H.; Park, J. W.; Lee, D.; Cho, N. K.; Kim, Y. S., Vertical Transport Control of Electrical Charge Carriers in Insulator/Oxide Semiconductor Hetero-structure. *Sci. Rep.* **2018,** *8*, 5643.

(11) Lee, D.; Park, J. W.; Cho, N. K.; Lee, J.; Kim, Y. S., Verification of Charge Transfer in Metal-Insulator-Oxide Semiconductor Diodes via Defect Engineering of Insulator. *Sci. Rep.* **2019,** *9*, 10323.

(12) Park, J. W.; Lee, D.; Cho, N. K.; Lee, J.; Kim, Y. S., Turn-On Voltage Shift of Metal-Insulator-Oxide Semiconductor Thin-Film Diode by Adding Schottky Diode in Reverse Direction. *ACS Appl. Electron Mater.* **2019,** *1* (4), 530-537.

(13) Hwang, H. Y.; Iwasa, Y.; Kawasaki, M.; Keimer, B.; Nagaosa, N; Tokura, Y., Emergent Phenomena at Oxide Interfaces. *Nat. Mater.* **2012,** *11*, 103-113.

(14) Yu, X.; Marks, T. J.; Facchetti, A., Metal Oxides for Optoelectronic Applications. *Nat. Mater.* **2016,** *15*, 383-396.

(15) Shriwastava, S.; Tripathi, C. C., Metal–Insulator–Metal Diodes: A Potential High Frequency Rectifier for Rectenna Application. *J. Electron. Mater.* **2019,** *48*, 2635-2652.

(16) Sze, S.M.; Ng, K. *Physics of Semiconductor Devices*, 3rd ed; John Wiley & Sons: Hoboken, NJ, 2006; Chapter 8, pp 448.

(17) Chiang, T. H.; Wager, J. F., Electronic Conduction Mechanisms in Insulators. *IEEE Trans. Electron Dev.* **2018,** *65* (1), 223-230.

(18) Lampert, M. A.; Mark, P., *Current injection in solids*. Academic Press: New York,, 1970; p xii, 351 p.

(19) Kao, K.-C., *Dielectric phenomena in solids : with emphasis on physical concepts of electronic processes*. Academic Press: Amsterdam ; Boston, 2004; p xvii, 581 p.

(20) Chiu, F. C., A Review on Conduction Mechanisms in Dielectric Films. *Adv. Mater. Sci. Eng.* **2014,** 578168 (2014).

Chapter 2 Electrical characteristics and rectification principle of MIOSM TFD using p-type oxide semiconductor

2.1 Overview

Oxide materials exhibiting transparency because of a bandgap wider than 3.0 eV have received considerable attention because they can demonstrate characteristics of not only a metal and a semiconductor but also an insulator[1]. These advantages have allowed the study of applying oxide materials to various devices such as solar cells, optical elements, displays, and gas sensors[2]. In recent years, next-generation memory or neuromorphic devices fabricated using oxide materials have received significant attention because they enable efficient and fast information processing because of the unique electrical properties of oxide materials[3-6]. Meanwhile, oxide thin-film transistors (TFTs) and oxide thin-film diodes (TFDs) with excellent electrical properties must be developed to operate those devices correctly in next-generation electronic circuits. TFTs using oxide materials have been developed intensively for more than a decade especially in the display field, because of their thinness, lightness, and excellent switching characteristics[7]. In recent years, even research on LTPO-based OLED TFTs,

combining the advantages of oxide and LTPS (low-temperature polycrystalline silicon) materials, has been reported to push the limits of oxide materials[8]. However, while oxide TFTs are being studied based on various oxide materials, developments related to oxide TFDs are relatively slow.

Conventional oxide TFDs have been manufactured in multiple forms using various oxide materials, such as contacting p-type and n-type oxide semiconductors (P–N junction) or contacting materials in a metal–insulator–metal (MIM) structure[9,10]. Nevertheless, oxide-based P–N diodes, MIM diodes, and Schottky diodes have shown limitations in electrical properties such as electrical instability, low rectification ratio, and narrow operating voltage range [11-14]. Oxide TFDs applied to next-generation electronic circuits must have stable rectification characteristics, convenient processes, and flexibility in the operating voltage range.

Recently, a new oxide TFD having excellent electrical properties has been reported, using the property that the charge carrier injected from the oxide semiconductor can pass through the inside of the insulator[15-18]. The metal–insulator–oxide semiconductor–metal (MIOSM) structure TFD exhibits rectifying properties by injecting or blocking charge carriers from the oxide semiconductor into trap states inside the insulator, depending on the voltage

difference between metal electrodes at both ends. Lampert et al. have reported that charge carriers injected from the outside can flow through trap states inside the insulator, and the density of the trap states determines the characteristics of the internal current[19-20]. Because the oxide semiconductor accumulates or depletes depending on the applied voltage, this property enables injecting or blocking charge carriers from the oxide semiconductor into the insulator. Therefore, based on the bulk engineering of the insulator and the interface engineering of the oxide semiconductor, the MIOSM TFD could have more excellent reliability, a higher rectification ratio, and a wider operating voltage range than the conventional oxide TFDs such as oxide-based P–N diodes, MIM diodes, and Schottky diodes.

On the other hand, all of the previously announced MIOSM TFDs have been fabricated based on n-type oxide materials[15-18]. When an insulator is deposited on the bottom metal, and an oxide semiconductor is deposited on the insulator, the current flow inside the insulator depends on the sign of the voltage applied to the bottom electrode. Accordingly, when an n-type semiconductor is applied for the diode, rectification occurs only in one direction. Therefore, the development of MIOSM TFDs with p-type oxide materials is essential for the flexibility of the electronic circuit configuration. In addition, to increase the scalability of new

TFDs, it is necessary to design materials that enable various specifications of diodes such as low-voltage driving, a high-voltage response, or a Zener diode as well as generic diodes.

Herein, we report for the first time MIOSM TFDs based on p-type oxide semiconductors. We used nickel oxide (NiO_X) as the p-type semiconductor, which is well known for its excellent thermal durability, chemical stability, low cost, and process convenience[22]. Contrary to the conventional n-type oxide, the new p-type oxide diode rectifies current based on the hole conduction inside the insulator. The behavior of electric charges inside the insulator and the rectification mechanism were analyzed based on the current density–voltage relationship of the diodes. Our new diodes show a stable rectification ratio of over 10^5 and have the advantage of selectively narrowing or widening the operating voltage range from ±8 to ±80 V. Consequently, the p-type MIOSM TFDs can overcome the limitations of the narrow operating voltage range, which was considered a disadvantage of conventional oxide diodes. We also confirmed the feasibility of the first transparent p-type MIOSM TFD by applying indium tin oxide (ITO) as an electrode. The new p-type NiO_X-based TFDs, capable of handling a low voltage as well as a high voltage, are expected to serve as a fundamental building block for next-generation electronic circuits along with n-type MIOSM TFDs.

2.2 Experimental Methods

2.2.1 Fabrication of p-type NiO_X-based MIOSM TFD

A highly doped Si wafer (resistivity < 0.005 Ω·cm) was used for the bottom metal of TFDs with a MIOSM structure. The Si wafer was washed sequentially for 15 min with detergent, 20 min with deionized (DI) water, 15 min with acetone, and 15 min with isopropyl alcohol (IPA) for surface cleaning. Subsequently, the wafer was dried with N2 gas, and surface impurities were removed for 2 min with atmospheric pressure plasma (APP, APP-02-HP, PSM inc.) equipment. SiO_2 and SiN_X layers were deposited by plasma-enhanced chemical vapor deposition (PECVD, PlasmaPro 100, Oxford instruments). The deposition conditions inside the PECVD chamber for SiO_2 are 1800 sccm for N_2O gas, 540 sccm for 5% SiH_4/N_2 gas, 1900 mTorr for working pressure, 140 W for high-frequency mode power, and 350 °C for substrate temperature. SiN_X conditions are 1000 sccm for N_2 gas, 34.5 sccm for NH_3 gas, 800 sccm for 5% SiH_4/N_2 gas, 1900 mTorr for working pressure, 270 W for high-frequency mode power, 400 W for low-frequency mode power, and 350 °C for substrate temperature. The NiO_X layer was prepared using a radio frequency (RF) magnetron sputtering system with a thickness of 70 nm and patterned using a 500 μm diameter shadow mask. The power applied to the NiO sputtering target was 100 W, and the pressure of O_2

inside the chamber was maintained at 1.0×10^{-2} Torr while NiO_X was deposited. The Ar/O_2 partial pressure inside the sputtering chamber was maintained at 0:10 mTorr, and the flow rate of oxygen gas was held at 10 sccm. Au was used for the top electrode on the oxide semiconductor layer, and the top electrode pattern with a diameter of 250 μm was deposited using a shadow mask. The Au electrode was deposited to a thickness of 100 nm using a thermal evaporation system. ITO was used as the bottom electrode for the transparent MIOSM TFD, and it was deposited to a thickness of 100 nm on a quartz substrate using a direct current (DC) magnetron sputtering system. Postannealing treatment was not applied to the fabrication of MIOSM TFD to increase the hole carrier concentration.

2.2.2 Characterizations

The current–voltage (I–V) relationship of the diodes was measured in the dark state and at room temperature using a semiconductor parameter analyzer (4155B, Agilent) and a probe station (MST 5500B, MSTech). High-resolution transmission electron microscopy (HR-TEM, JEOL, JEM-2100F) and focused ion beam (FIB, Quanta 3D FEG, FEI) were used to observe the vertical cross section of the p-type MIOSM TFD.

2.3 Charge transport mechanism in the p-type MIOSM TFD

Figure 1 shows schematic illustrations of two types of diode structures and their vertical current-voltage (*I-V*) measurements. Both diodes used 70-nm-thick p-type NiO_X as an oxide semiconductor layer. Heavily boron-doped (p^{++}) Si and Au were applied to the top and bottom electrodes of both diodes. Detailed methods are provided in the experimental section. The difference between the TFD structure of Figure 2.1(a) and Figure 2.1(b) is the presence of 100-nm-thick SiO_2. Metal-oxide semiconductor-metal (M-OS-M) structure without SiO_2 layer forms typical Schottky contact at each M-OS interface (p^{++} Si/NiO_X and Au/NiO_X). When the top electrode was fixed at 0 V, and the bottom electrode was swept from -4 V to 4 V, the rectification ratio of the Schottky diode was 6 at ±2 V (Figure 2.2(a)). In contrast, a MIOSM diode of a metal insulator-oxide semiconductor-metal (M-I-OS-M) structure with 100-nm-thick SiO_2 (Figure 2.3) exhibited significantly different *I-V* characteristics than the Schottky diode. The rectification ratio of the MIOSM TFD was 2.2×10^5 at ±20 V, which is ~10^5 times more than that of the Schottky diode (Figure 2.2(b)). In particular, it was confirmed that when the bottom electrode was negatively biased, current flew effectively from top to bottom, and when positively biased, the current did not

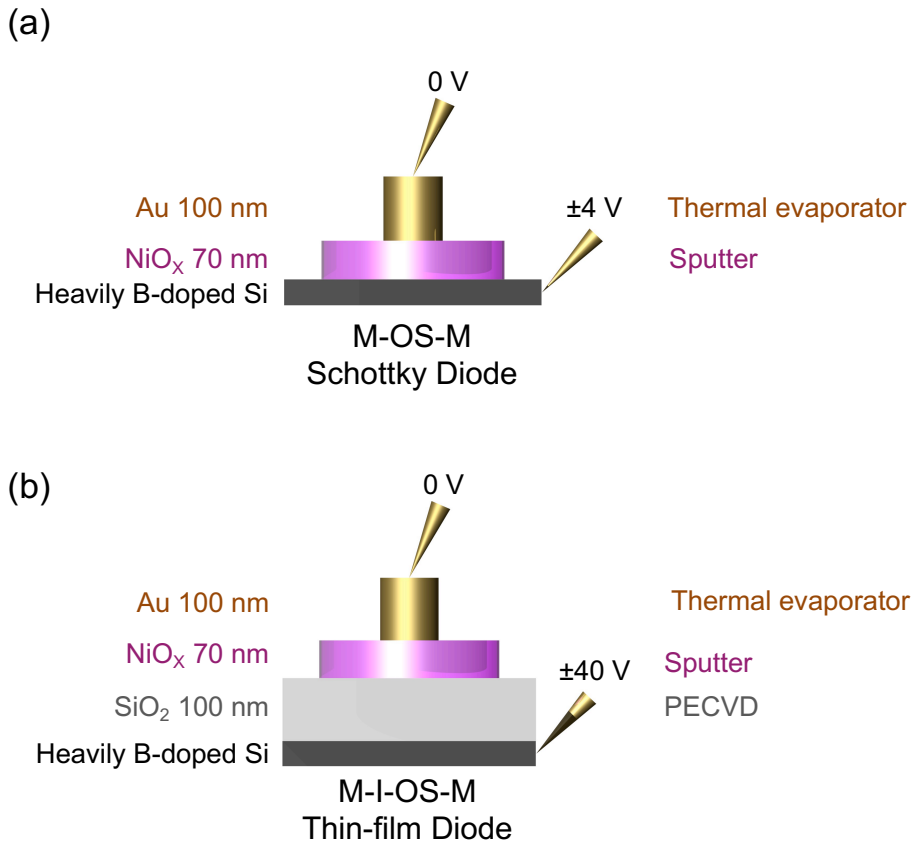

Figure 2.1. Fabrication of p-type NiO_X-based (a) Schottky diode and (b) MIOSM Thin-film Diode (TFD).

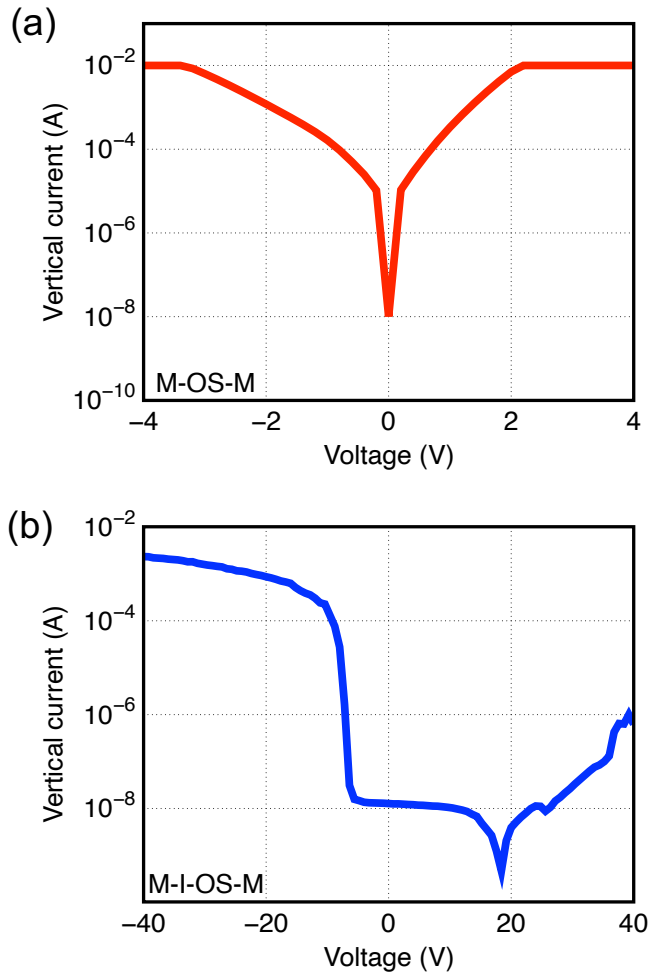

Figure 2.2. (a) Vertical current-voltage (*I-V*) relationship of the Schottky diode.

(b) *I-V* relationship of p-type NiO_X-based MIOSM TFD with the SiO_2 layer.

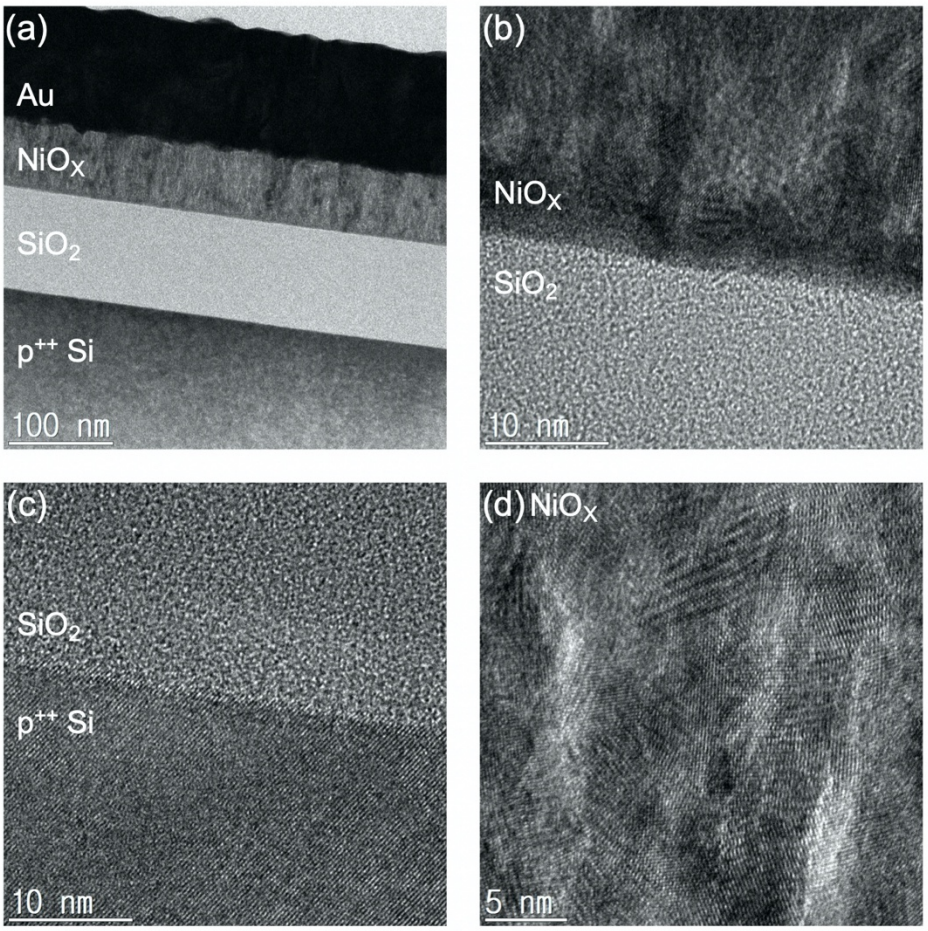

Figure 2.3. Cross-sectional high-resolution transmission electron microscopy (HRTEM) image of (a) heavily boron-doped (p^{++}) Si/100-nm-thick SiO_2/70-nm thick NiO_X/100-nm-thick Au structure metal-insulator-oxide semiconductor-metal (MIOSM) thin-film diode (TFD), (b) the interface between SiO_2 and NiO_X, (c) the boundary between p^{++} Si and SiO_2, and (d) polycrystalline NiO_X film.

flow relatively. This is the first report of the p-type MIOSM TFD, and the new type of diode has the advantage that it can provide stable rectification characteristics by simply inserting an insulator (SiO_2) between the p-type oxide semiconductor (NiO_X) and the bottom electrode (p^{++} Si).

To analyze the on-state conduction mechanism of the p-type MIOSM TFD, the vertical current density-negative voltage (*J-V*) was plotted and fitted on a log-log scale (Figure 2.4(a)). The fitting value of the slope showed the typical current mechanism of space-charge-limited conduction (SCLC). As reported by MA Lampert et al., the SCLC region consists of a traps-filled-limit (TFL) current region that describes the behavior of charge carriers moving while filling the trap states inside the insulator, and a Child's law region that describes the behavior after filling the trap states[22]. This result indicates that, depending on the voltage applied to the bottom electrode (hole collecting contact), holes in NiO_X are injected into the traps inside the SiO_2 layer, and flow toward the bottom electrode (hole injecting contact). When the bottom electrode (p^{++} Si) is negatively biased, and the top electrode (Au) is grounded, holes accumulate from the SiO_2/NiO_X interface to the inside of the NiO_X layer (Figure 2.4(b)). However, even if a negative bias is applied to the bottom electrode, carriers accumulated at the NiO_X

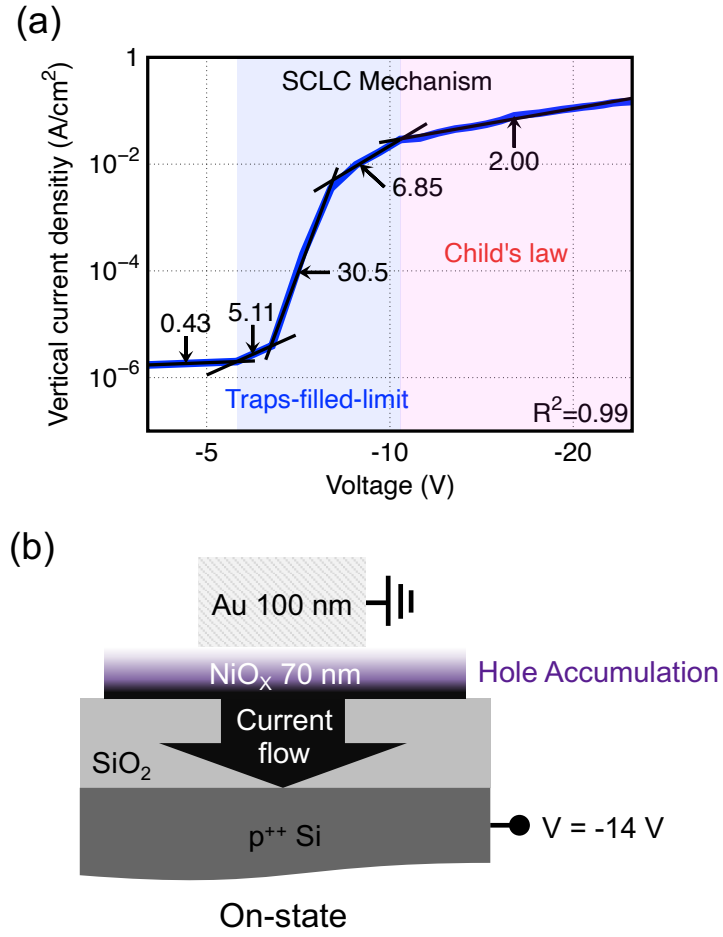

Figure 2.4. (a) Vertical current density-voltage (*J-V*) plot and fitting curves to verify space-charge-limited conduction (SCLC) in the SiO_2 layer with trap states. (b) Schematic of current flow inside the SiO_2 layer according to the hole accumulation and injecting at the NiO_X surface.

do not immediately pass through SiO_2 layer (off-state, slope < 1). When the density of thermally generated free carriers in SiO_2 (p_0) is greater than the density of carriers injected into SiO_2 (p_i), traps are partially filled by very weak injection (Figure 2.5(a), $p_i < p_0$). Therefore, the dielectric relaxation time (τ_d) is shorter than the carrier transit time (τ_c), and the accumulated carriers cannot pass through SiO_2 layer (Figure 2.5(b), $\tau_d < \tau_c$). As the negative bias increases, holes accumulated at the NiO_X surface are strongly injected into the trap states in SiO_2.

While the density of the strongly injected carrier increases, the carrier transit time in SiO_2 becomes shorter than the dielectric relaxation time ($\tau_c < \tau_d$), and density of unfilled traps starts to decrease (Figure 2.6(a)). The J_{TFL}-V property associated with TFL behavior can be expressed by the following equation[22]:

$$J_{TFL} = \frac{9}{8}\varepsilon\mu_p\theta_a\frac{V^2}{d^3} \quad (1)$$

where ε is the dielectric constant, μ_p is the hole mobility, d is the thickness of the insulator, and θ_a is the ratio of the free carrier density to total carrier density. θ_a is given by

$$\theta_a = \frac{p}{p + p_t} \quad (2)$$

where p is the density of injected free holes, and p_t is the density of trapped holes. Although the quasi-Fermi level (E_{Fp}) is still above the hole trapping level (E_t), the strongly injected carriers begin to dominate the thermally generated

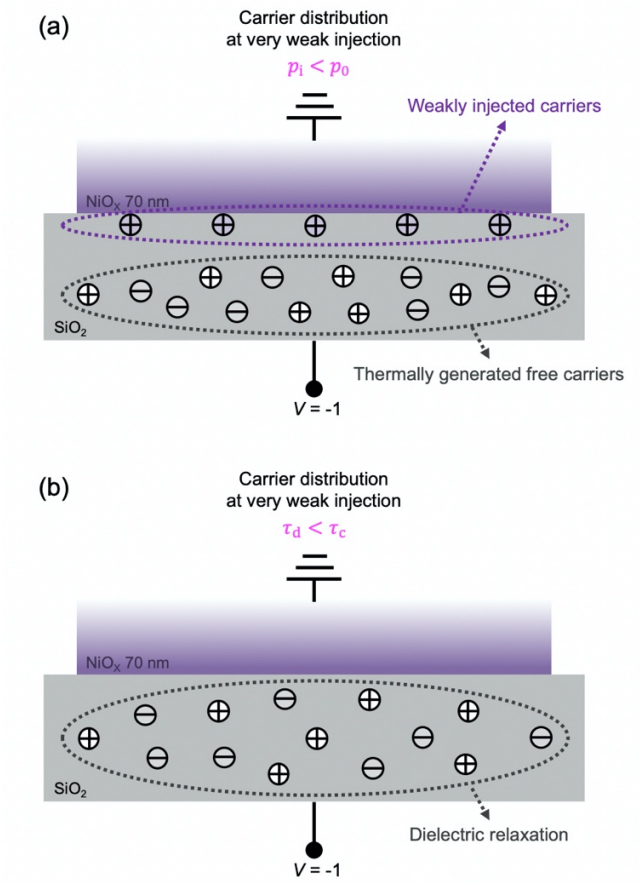

Figure 2.5. (a) Schematic figures illustrating carrier distribution inside the SiO_2 layer when the hole carriers are weakly injected from the p-type nickel oxide (NiO_X) to the trap states inside the SiO_2 layer. (b) Charge redistribution when the carrier transit time of weakly injected holes (τ_c) is longer than the dielectric relaxation time (τ_c). When the density of injected carrier (p_i) is smaller than the of thermally generated free carrier (p_0) in equilibrium, dielectric layer has a tendency to maintain the charge neutrality and it is called dielectric relaxation.

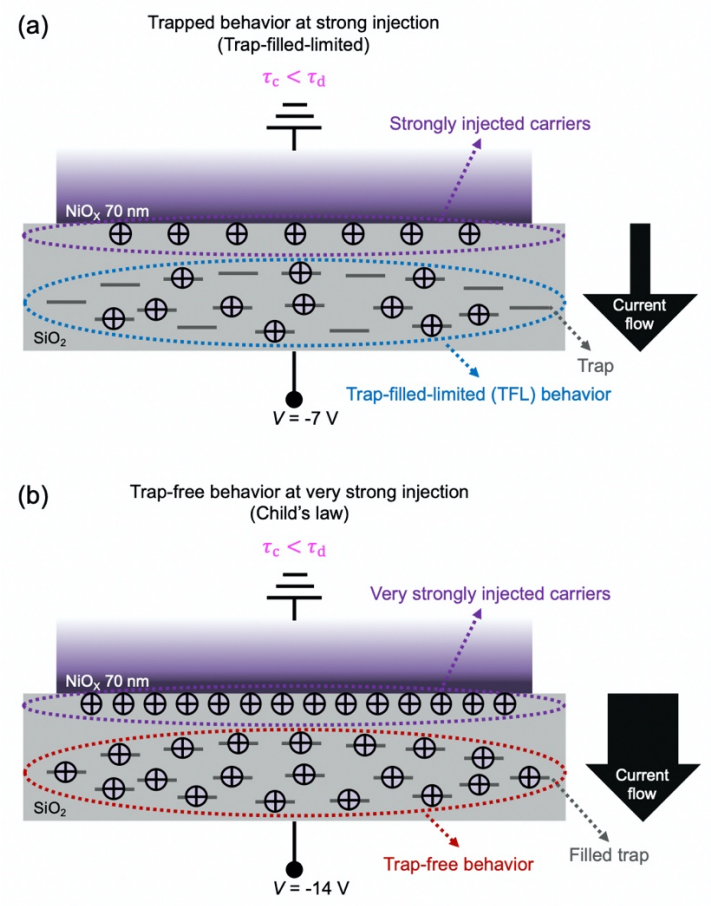

Figure 2.6. (a) Graphical schematic for the charge carrier behavior inside the SiO_2 layer when the carrier transit time of strongly injected holes (τ_c) is shorter than the dielectric relaxation time (τ_c). As strongly injected carriers fill the trap states inside the insulator, they exhibit traps-filled-limited (TFL) behavior. (b) Very strongly injected carriers show trap-free behavior after filling all trap states inside the SiO_2 layer and follow Child's law.

carrier, and the vertical current increases rapidly as the carriers exhibit TFL behavior (slope $>$ 2). When the voltage applied to the bottom electrode increases more than traps-filled-limit voltage (V_{TFL}), conduction follows the trap-free SCLC (Child's law) as all traps are filled with a very strong injection (Figure 2.6(b)), and the p_t becomes 0. As a result, θ_a turns into 1 in the equation (1), and the following equation can express the J_{Child}-V property associated with trap-free SCLC behavior[22]:

$$J_{\mathrm{Child}} = \frac{9}{8}\varepsilon\mu_{\mathrm{p}}\frac{V^2}{d^3} \quad (3)$$

At voltages above V_{TFL} where E_{Fp} passes the E_t, log J_{Child} is proportional to 2log V, according to equation (3). The relationship was verified in the Child's law part of Figure 2.4(a) (slope ~ 2). These results indicate that the NiO_X-based p-type MIOSM TFD's on-state current depends on the injection of holes from NiO_X (electrode-limited conduction mechanism) and property of trap states in SiO_2 (bulk-limited conduction mechanism).

On the other hand, to understand how the TFD maintains off-state, the relationship between vertical current density-positive voltage (J-V) was plotted on a log-log scale. The graph could be divided into two parts: one part in which the J decreased as the V increased, and the other part in which the J increased as the V increased (Figure 2.7(a)). While the J decreases as the V increases,

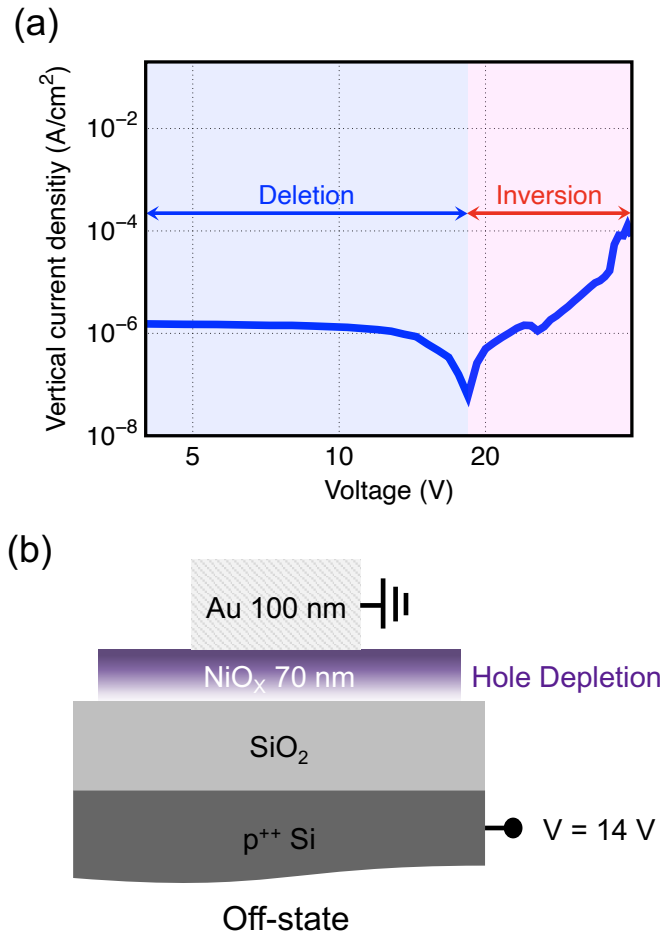

Figure 2.7. (a) *J-V* relationship showing depletion and inversion of the NiO_X surface. (b) Schematic of blocking hole injection into the SiO_2 layer due to hole depletion of the NiO_X surface.

the p-type oxide semiconductor depletes at the SiO_2/NiO_X interface (Figure 2.7(b)). When NiO_X surface is depleted, the carrier cannot be injected into SiO_2 layers from NiO_X semiconductor and consequently, there is no external carrier passing through SiO_2 layer. As the positive V continuously increases at the bottom electrode, the E_{Fp} eventually draws level with the intrinsic Fermi level (E_{Fi}) at a specific voltage, so that the vertical current density exhibits minimum. After this transition point, the E_{Fp} passes the E_{Fi}, and the NiO_X surface becomes an inversion state at the SiO_2/NiO_X interface. As a result, electron concentration increases at the NiO_X surface. When we keep increasing the positive voltage, more inverted electrons induce injecting carriers into the trap states of SiO_2, which leads to an increase in the off-current of the diode. These results show that the MIOSM TFD's off-state current is affected by the depletion/inversion at the NiO_X surface (electrode-limited conduction mechanism) and defect properties in the SiO_2 layer (bulk-limited conduction mechanism).

2.4 Selectable operating voltage and high withstand voltage.

Meanwhile, since the electronic circuit uses various voltage ranges from low to high voltage, diode specifications corresponding to various operating voltage ranges are required. Therefore, in order to broadly expand the application range

of MIOSM TFD, it is essential to produce a diode having an operating voltage range suitable for a specific condition. One of the notable advantages of the MIOSM TFD is that the operating voltage range can be adjusted by selectively changing the insulator thickness. This is due to the phenomenon that the carriers follow the SCLC mechanism as they flow through the trap states inside the insulator. According to the SCLC mechanism, as shown in equations (1) and (3), the current density can increase when the thickness decreases at the same voltage. Therefore, by reducing the insulator's thickness, the diode can exhibit a relatively high amount of current even at a low voltage. Conversely, by increasing the thickness, the diode can operate at a relatively high voltage. Therefore, by employing the bulk-limited conduction mechanism of the insulator, it is possible to produce oxide TFDs that can selectively set the operating voltage region.

In order to verify whether operating voltage range can be adjusted according to the insulator thickness control in the p-type MIOSM TFD, diodes were fabricated by splitting the thickness of SiO_2 into 10, 25, and 100 nm. The deposition condition of the p-type NiO_X was the same for all cases. Figure 2.8(a) shows that the diode's operating voltage range effectively changes as the SiO_2 thickness variations. As the thickness became thinner from 100 nm to 10 nm, the current tended to increase at the same voltage, and the diode's operating voltage range

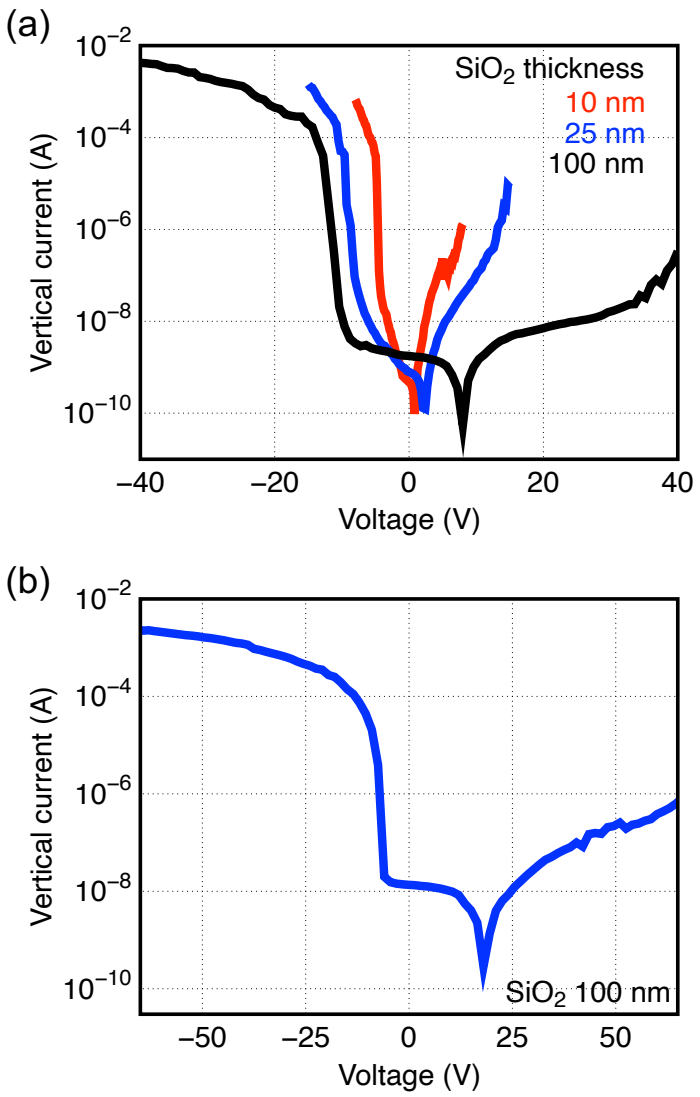

Figure 2.8. (a) *I-V* relationship showing that the operating voltage region of p-type NiO_X-based MIOSM TFD can be selectively adjusted according to SiO_2 thickness variation. (b) *I-V* relationship of p-type NiO_X-based MIOSM TFD showing stable driving in the high voltage range.

began to narrow. The reason for these results is that the injected carriers flow through the trap states inside the insulator. As the thickness of SiO_2 decreases, the total length that the carrier passes also decreases. Therefore, the total amount of carriers injected to fill all trap states reduces with decreasing thickness of SiO_2. When the current density by the thermally generated free carrier in SiO_2 is equal to the current density by the carrier injected from NiO_X, the current begins to flow through SiO_2 layer according to the TFL behavior represented by equation (1). From this moment, the MISOM TFD turns on, and the diode's turn-on voltage (V_{on}) can be defined as follows[22]:

$$V_{on} = -\frac{8}{9}\frac{qp_0d^2}{\theta_a\varepsilon} \quad (4)$$

where q is the electric charge of the hole. According to equation (4), the V_{on} gets closer to 0 V as the insulator's thickness decreases. As a result, when the insulator becomes thinner, the injected carrier exhibits trap-free behavior faster. Conversely, when the insulator gets thicker, the injected carrier shows a trap-free SCLC at a higher voltage. Consequently, thick insulator-based diodes have a wider operating voltage range than thin insulator-based diodes. Figure 2.8(b) shows that, when SiO_2 has a thickness of 100 nm, the diode functioned stably in the higher voltage ranges from -65 V to 65 V. In addition, when a voltage of 100 V was applied to the bottom electrode, the diode was able to withstand even 80

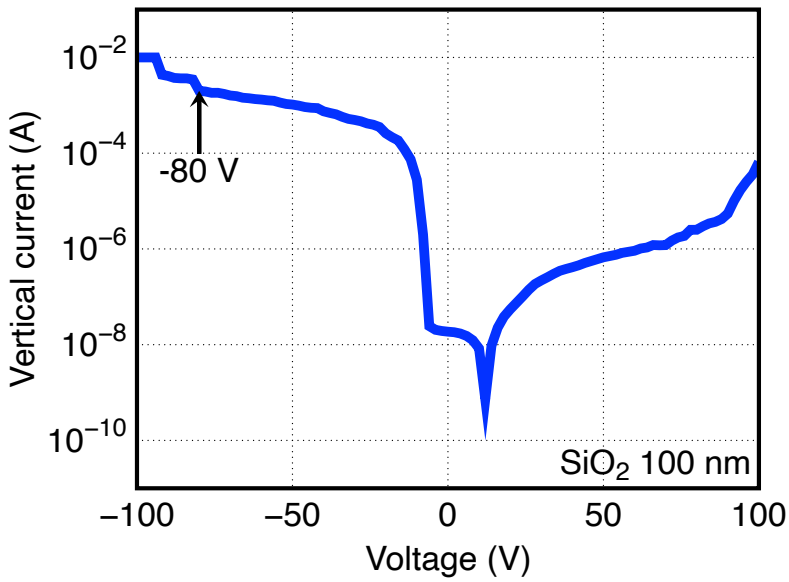

Figure 2.9. High-voltage withstand and electrical breakdown test for a MIOSM TFD based on p-type NiO_X with 100-nm thick SiO_2. The TFD showed a breakdown at -80 V when ±100 V was applied to the bottom electrode.

V (Figure 2.9). These results show the advantage of MIOSM TFD, which can produce diodes for high-voltage devices as well as diodes for low-voltage electronics by simply adjusting the thickness of the insulator.

2.5 Insulator changeability and transparency of MIOSM TFD

As described above, in the case of MIOSM TFDs, after the carriers fill the trap states inside the insulator, they show trap-free conduction. In general, except for the ideal case, all insulators have trap states within that act as a charge transfer path[22,23]. Therefore, the characteristics of MIOSM TFD depend not only on the electrical characteristics of the electrode and oxide semiconductor (electrode-limited conduction mechanism) but also on the insulator's thickness and trap states (bulk-limited conduction mechanism). Hence, one of the other advantages of MIOSM TFD is that the diode's electrical characteristics can be changed by varying the insulator. Figure 2.10(a) shows the advantage of the diode. Instead of SiO_2 layer, 100 nm-thick SiN_X was deposited by plasma-enhanced chemical vapor deposition (PECVD) as the charge transfer path. SiN_X-based TFD also displayed stable rectification characteristics from -65 V to 65 V, similar to SiO_2-based, and the rectification ratio of the diode was about 10^4 at ±65 V (Figure 2.10(b)). In addition, carriers injected from the outside filled the trap states inside

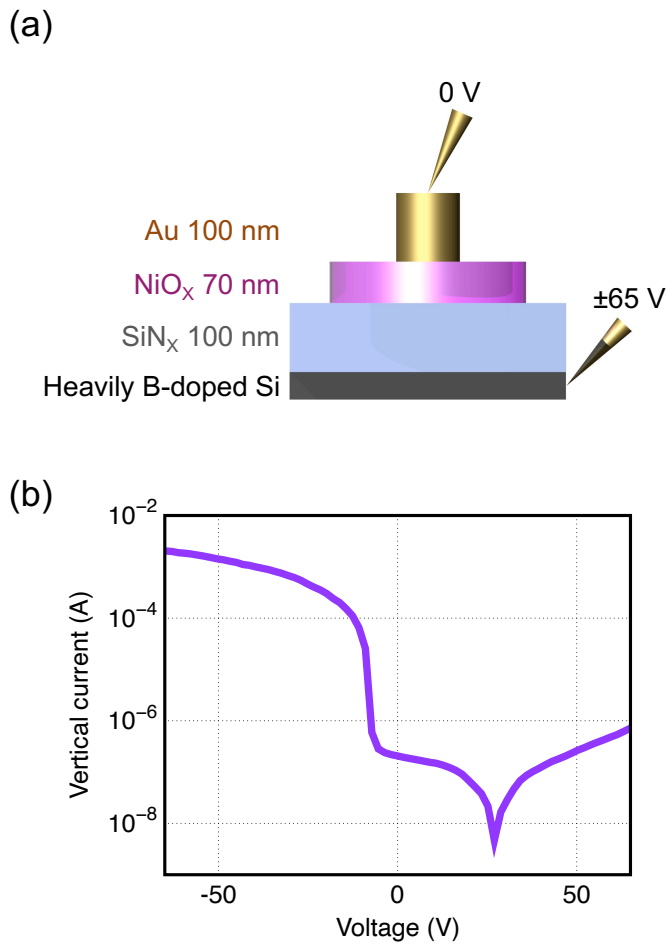

Figure 2.10. (a) Schematic figures illustrating the device structures and (b) *I-V* characteristics of the heavily boron-doped Si/SiN_X/NiO_X/Au structure.

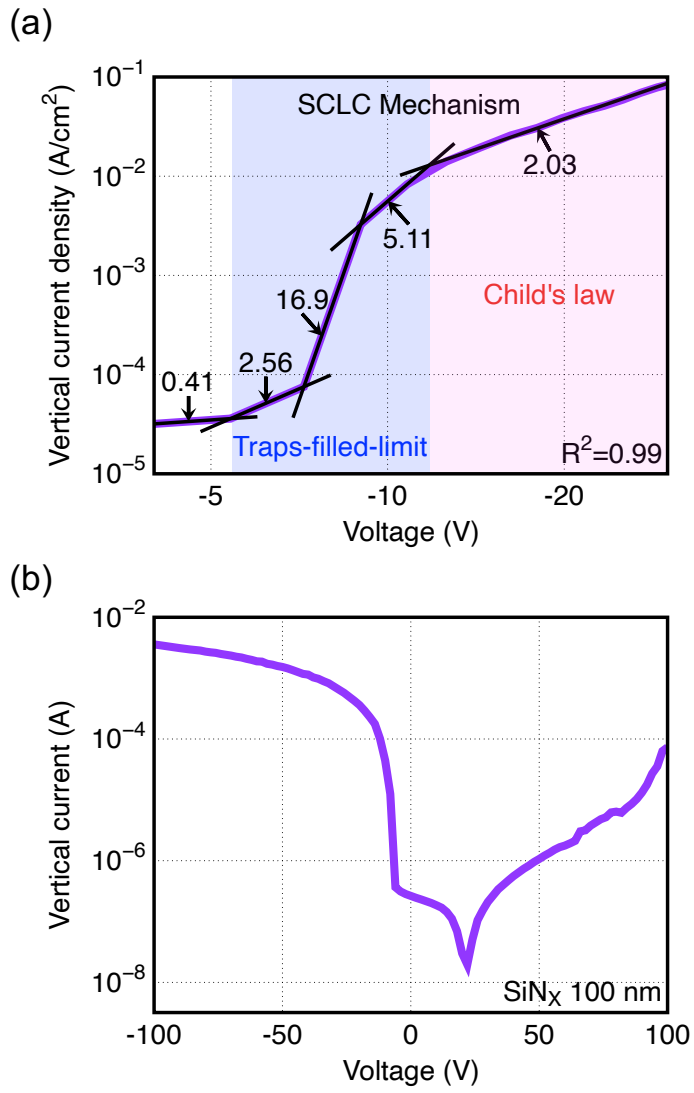

Figure 2.11. (a) Log-log relation between vertical current density and voltage characteristics for space-charge-limited conduction (SCLC) in the heavily boron-doped Si/SiN_X/NiO_X/Au structure MIOSM TFD. The charge transfer mechanism is divided into one part in which charge carriers injected from NiO_X surface into

the trap states of the SiN_X layer move while filling the traps (Traps-filled-limit), and the other part which indicates the trap-free behavior when the carriers move without trapping (Child's law). (b) High-voltage withstand test for p-type NiO_X MIOSM TFD with 100-nm thick SiN_X. The TFD did not breakdown when biased from -100 V to 100 V.

SiN_X first (traps-filled-limit), and then showed trap-free behavior (Child's law), which confirms that the carrier conduction follows the SCLC mechanism (Figure 2.11(a)). Figure 2.11(b) shows that when the SiN_X is 100 nm thick, the diode operates reliably without a breakdown in the high voltage range of -100 V to 100 V. Therefore, it is considered that various insulators can be used as a carrier transport layer of p-type MIOSM TFD by securing a method of controlling the trap states the insulators depending on the purpose.

Oxide materials not only offer excellent electrical properties from metal to insulator but also have the advantage of being transparent[1]. Therefore, a high-performance oxide-based TFD is necessary as a fundamental element in a next-generation transparent electronic circuit. However, p-type oxide-based transparent MIOSM TFD has not been reported yet. We confirmed the feasibility of a transparent p-type MIOSM TFD for the first time by replacing the p^{++} Si bottom electrode with a transparent ITO (Figure 2.12(a)). ITO was deposited on a quartz glass by direct current sputtering system, and Au was deposited by thermal evaporation system. The reason for adopting Au without making an all-transparent diode using ITO as the top electrode is that ITO forms a Schottky contact with NiO_X, while Au forms an ohmic contact[24,25]. Transparent diode using 100-nm-thick SiO_2 showed stable rectification characteristics when the bottom

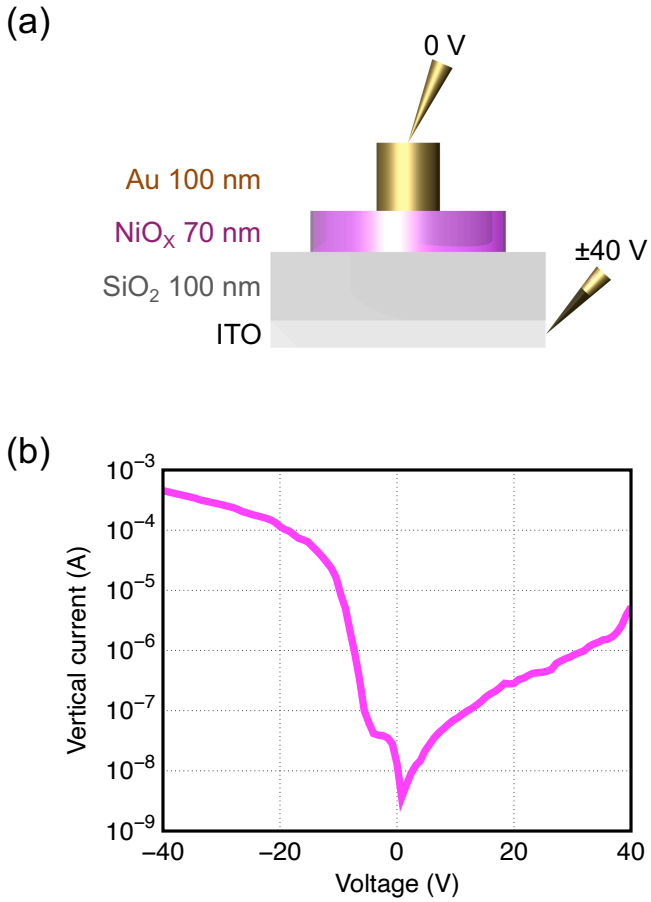

Figure 2.12. (a) Schematic figures illustrating the device structures and (b) *I-V* characteristics of the transparent ITO/SiO_2/NiO_X/Au structure MIOSM TFD.

electrode was biased from -40 V to 40 V, and the rectification ratio was ~10^4 at ±20 V (Figure 2.12(b)). The transparent diode also showed TFL conduction as the holes filled the trap states inside the SiO_2 and followed Child's law after the traps were filled (Figure 2.13). Based on the optimization of trap states of various insulators and the electrical properties of oxide semiconductors, transparent p-type oxide-based MIOSM TFD is expected to be effectively used in circuits applied to next-generation electronic devices.

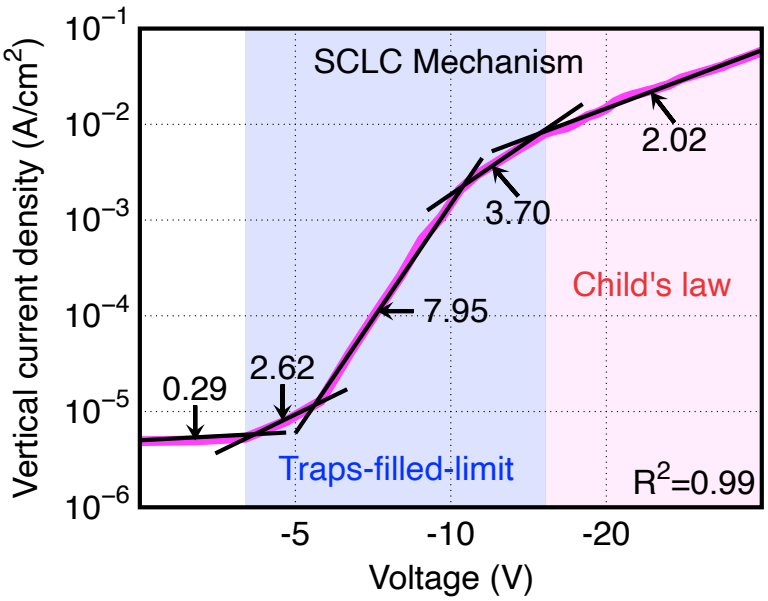

Figure 2.13. Log-log relation between vertical current density and voltage characteristics for space-charge-limited conduction (SCLC) in the transparent ITO/SiO_2/NiO_X/Au structure MIOSM TFD.

2.6 Conclusion

In summary, we demonstrated the first MIOSM TFD using p-type NiO_X and investigated the diode's rectification principle. The Schottky diode using p-type NiO_X had a rectification ratio of only 6 at ±2 V, but when 100-nm-thick SiO_2 with trap states was inserted between the p-type NiO_X and the bottom electrode, the diode showed a high rectification ratio of 2.2×10^5 at ±20 V. The fitting result of the *J-V* relationship confirmed that the SCLC mechanism could explain the behavior of carriers moving through the trap states inside SiO_2 layer. The carriers injected from NiO_X moved to the bottom electrode while filling trap states inside the insulator (traps-filled-limit) and exhibited trap-free conduction after filling the trap states (Child's law). The electrical characteristics also confirmed that the MIOSM TFD could remain off-state because the carrier could not move into the insulator's trap states as the NiO_X surface depleted. The operating voltage range of the diode was determined by adjusting the thickness of the insulator. It was possible to fabricate a low voltage driving diode using a thin insulator and a high voltage driving diode using a thick insulator. The MIOSM TFD that changed the type of insulator from SiO_2 to SiN_X demonstrated the expandability of the diode, and the p-type diode with the ITO bottom electrode confirmed that manufacturing a transparent MIOSM TFD is possible. The p-type MIOSM TFD is expected to

be a fundamental building block for next-generation transparent circuits as research extends to optimize carrier injection and depletion of various oxide semiconductors and efficiently control the trap states of various insulators.

2.7. Reference

(1) Hosono, H., Recent progress in transparent oxide semiconductors: Materials and device application. *Thin Solid Films* **2007,** *515* (15), 6000-6014.

(2) Yu, X. G.; Marks, T. J.; Facchetti, A., Metal oxides for optoelectronic applications. *Nat. Mater.* **2016,** *15* (4), 383-396.

(3) Jo, S. H.; Chang, T.; Ebong, I.; Bhadviya, B. B.; Mazumder, P.; Lu, W., Nanoscale Memristor Device as Synapse in Neuromorphic Systems. *Nano Lett.* **2010,** *10* (4), 1297-1301.

(4) Waser, R.; Aono, M., Nanoionics-based resistive switching memories. *Nat. Mater.* **2007,** *6* (11), 833-840.

(5) Kim, M. K.; Lee, J. S., Synergistic Improvement of Long-Term Plasticity in Photonic Synapses Using Ferroelectric Polarization in Hafnia-Based Oxide-Semiconductor Transistors. *Adv. Mater.* **2020,** *32* (12), e1907826.

(6) Lyu, B.; Choi, Y.; Jing, H.; Qian, C.; Kang, H.; Lee, S.; Cho, J. H., 2D MXene-TiO_2 Core-Shell Nanosheets as a Data-Storage Medium in Memory Devices. *Adv. Mater.* **2020,** *32* (17), e1907633.

(7) Fortunato, E.; Barquinha, P.; Martins, R., Oxide Semiconductor Thin-

Film Transistors: A Review of Recent Advances. *Adv. Mater.* **2012,** *24* (22), 2945-2986.

(8) Shim, G. W.; Hong, W.; Cha, J. H.; Park, J. H.; Lee, K. J.; Choi, S. Y., TFT Channel Materials for Display Applications: From Amorphous Silicon to Transition Metal Dichalcogenides. *Adv. Mater.* **2020,** *32,* e1907166.

(9) Narushima, S.; Mizoguchi, H.; Shimizu, K.; Ueda, K.; Ohta, H.; Hirano, M.; Kamiya, T.; Hosono, H., A p-type amorphous oxide semiconductor and room temperature fabrication of amorphous oxide p-n heterojunction diodes. *Adv. Mater.* **2003,** *15* (17), 1409-1413.

(10) Cowell, E. W.; Alimardani, N.; Knutson, C. C.; Conley, J. F.; Keszler, D. A.; Gibbons, B. J.; Wager, J. F., Advancing MIM Electronics: Amorphous Metal Electrodes. *Adv. Mater.* **2011,** *23* (1), 74-78.

(11) Marques, G. C.; Tahoori, M.; Aghassi-Hagmann, J.; Sukuramsyah, A. M.; Rus, A. A.; Bolat, S.; Aribia, A.; Feng, X. W.; Singaraju, S. A.; Ramon, E.; Romanyuk, Y., Fabrication and Modeling of pn-Diodes Based on Inkjet Printed Oxide Semiconductors. *IEEE Electr. Device L.* **2020,** *41* (1), 187-190.

(12) Periasamy, P.; Berry, J. J.; Dameron, A. A.; Bergeson, J. D.; Ginley,

D. S.; O'Hayre, R. P.; Parilla, P. A., Fabrication and Characterization of MIM Diodes Based on Nb/Nb_2O_5 Via a Rapid Screening Technique. *Adv. Mater* **2011,** *23* (27), 3080-3085.

(13) Urcuyo, R.; Duong, D. L.; Jeong, H. Y.; Burghard, M.; Kern, K., High Performance Graphene-Oxide-Metal Diode through Bias-Induced Barrier Height Modulation. *Adv. Electron Mater.* **2016,** *2* (9), 1600223.

(14) Son, Y.; Li, J. B.; Peterson, R. L., In Situ Chemical Modification of Schottky Barrier in Solution Processed Zinc Tin Oxide Diode. *ACS Appl. Mater. Inter.* **2016,** *8* (36), 23801-23809.

(15) Lee, E.; Lee, J.; Kim, J. H.; Lim, K. H.; Byun, J. S.; Ko, J.; Kim, Y. D.; Park, Y.; Kim, Y. S., Direct electron injection into an oxide insulator using a cathode buffer layer. *Nat. Commun.* **2015,** *6,* 1-6.

(16) Lee, J.; Yoon, K.; Lim, K. H.; Park, J. W.; Lee, D.; Cho, N. K.; Kim, Y. S., Vertical Transport Control of Electrical Charge Carriers in Insulator/Oxide Semiconductor Hetero-structure. *Sci. Rep.* **2018,** *8*, 5643.

(17) Lee, D.; Park, J. W.; Cho, N. K.; Lee, J.; Kim, Y. S., Verification of Charge Transfer in Metal-Insulator-Oxide Semiconductor Diodes via Defect Engineering of Insulator. *Sci. Rep.k* **2019,** *9*, 10323.

(18) Park, J. W.; Lee, D.; Cho, N. K.; Lee, J.; Kim, Y. S., Turn-On Voltage Shift of Metal-Insulator-Oxide Semiconductor Thin-Film Diode by Adding Schottky Diode in Reverse Direction. *ACS Appl. Electron Mater.* **2019,** *1* (4), 530-537.

(19) Chiang, T. H.; Wager, J. F., Electronic Conduction Mechanisms in Insulators. *IEEE Trans. Electron Dev.* **2018,** *65* (1), 223-230.

(20) Lampert, M. A.; Mark, P., *Current injection in solids*. Academic Press: New York,, 1970; p xii, 351 p.

(21) Sajid, S.; Elseman, A. M.; Huang, H.; Ji, J.; Dou, S. Y.; Jiang, H. R.; Liu, X.; Wei, D.; Cui, P.; Li, M. C., Breakthroughs in NiOx-HTMs towards stable, low-cost and efficient perovskite solar cells. *Nano Energy* **2018,** *51*, 408-424.

(22) Kao, K.-C., *Dielectric phenomena in solids : with emphasis on physical concepts of electronic processes*. Academic Press: Amsterdam ; Boston, 2004; p xvii, 581 p.

(23) Chiu, F. C., A Review on Conduction Mechanisms in Dielectric Films. *Adv. Mater. Sci. Eng.* **2014,** 578168 (2014)

(24) Irwin, M. D.; Buchholz, B.; Hains, A. W.; Chang, R. P. H.; Marks, T.

J., p-Type semiconducting nickel oxide as an efficiency-enhancing anode interfacial layer in polymer bulk-heterojunction solar cells. *Proc. Natl. Acad. Sci. U.S.A* **2008,** *105* (8), 2783-2787.

(25) Irwin, M. D.; Servaites, J. D.; Buchholz, D. B.; Leever, B. J.; Liu, J.; Emery, J. D.; Zhang, M.; Song, J. H.; Durstock, M. F.; Freeman, A. J.; Bedzyk, M. J.; Hersam, M. C.; Chang, R. P. H.; Ratner, M. A.; Marks, T. J., Structural and Electrical Functionality of NiO Interfacial Films in Bulk Heterojunction Organic Solar Cells. *Chem. Mater.* **2011,** *23* (8), 2218-2226.

Chapter 3 Turn-on Voltage Shift of Metal-Insulator-Oxide Semiconductor Thin-Film Diode by Adding Schottky Diode in Reverse Direction

3.1 Overview

High capacitance and low leakage are guaranteed in insulators with relatively low thicknesses with the introduction of high-κ materials in metal-insulator-metal (MIM) capacitors or metal-oxide-semiconductor (MOS) electronics applications.[1,2] However, when the insulator thickness is reduced to a few nanometers, electrons in a device made of a high-κ material are more likely to pass through a thin insulator by means of quantum tunneling and to move along internal trap and/or defect states. In order to overcome this limitation, various methods have been proposed to minimize insulator trap and defect states.[3] In contrast, utilizing the charge transfer effect through an insulator a few nanometers thick has also been noted for decades due to the high applicability of this method to various electronic devices such as MIM diodes.[4] Combining multiple materials to increase the rectification ratio of MIM diodes has also been attempted. Examples include the metal-insulator-insulator-metal (MIIM) and graphene-insulator-metal (GrIM) configurations.[5,6] When the electrical characteristics of

the electrode-dielectric contact determine the behavior of the charge, the MIM diode follows one of a number of electrode-limited transport mechanisms. These are (1) Schottky or thermionic emission, (2) Fowler-Nordheim tunneling, (3) direct tunneling, or (4) thermionic-field emission.[7]

Studies using traps or defect states as charge transfer paths in insulators for devices with MIM structures have drawn attention in relation to research areas such as resistive random-access memory (RRAM) and MOS photoelectrodes.[8,9,10] When electrons pass through the insulator under the influence of trap or defect states in the insulator, they follow a bulk conduction mechanism such as Poole-Frenkel emission, hopping conduction, ohmic conduction, space-charge-limited conduction, ionic conduction, or grain-boundary-limited conduction.[7] Various types of trap or defect engineering have been attempted to improve device performance capabilities by optimizing the trap or defect states of an insulator, but it remains challenging to reproduce the density or distribution of trap or defect states uniformly in a thin insulator.[11,12] However, these obstacles can be reduced by increasing the thickness of the insulator having significant trap or defect states to approximately several tens of nanometers or more.[13,14,15] When voltage is applied to a MIM device with a relatively thick insulator, the charge moves in the insulator due to the electrical characteristics of the metal-insulator contacts and

the trap or defect properties of the insulator. This charge flow is referred to as leakage current in metal-oxide-semiconductor-field-effect transistors (MOSFETs), which are considered to be better devices when these types of flows do not occur. However, when many trap or defect states initially or artificially exist in an insulator, the charge can be uniformly transferred even in a relatively thick insulator of several tens of nanometers or more.

Using these characteristics, a new concept of a thin-film diode (TFD) has been developed recently with superior stability and a high rectification ratio in metal-insulator-oxide semiconductor (MIOS) structures with relatively thick insulators. Choi et al. have shown high performance all transparent TFDs with 50 nm insulator.[13,14] Lee et al. also reported a TFD with relatively thick insulator (>100 nm).[15] Both novel TFDs have low leakage current density under 10^{-9} A/cm^2 and a high rectifying ratio of 10^8–10^9. The MIOS TFD can be manufactured with simple processes, and the rectification ratio can easily be controlled by changing the electron mobility or doping level of the oxide semiconductor. The novel MIOS TFD has rectifying characteristics according to the accumulation or depletion principle of the oxide semiconductor on the insulator side due to the voltage difference between the metal and the oxide semiconductor. A TFD with the MIOS structure follows the electrode-limited conduction mechanism because it exhibits

rectification characteristics due to the injection and blocking of the charge generated in the insulator-semiconductor junction. Moreover, the MIOS TFD follows a bulk-limited conduction mechanism because the current characteristics of the device are affected by the trap or defect states of the insulator and the applied voltage. The MIOS structure and new rectification mechanism of the novel TFD can be a great advantage to replace conventional p-n type TFDs, which are difficult to manufacture due to the absence of stable p-type oxide semiconductors and have a low rectifying ratio.[16]

However, the MIOS TFD requires further research on turn-on voltage control to broaden the various specifications and simplify the circuit design to be applied. All MIOS TFDs reported thus far have characteristics that turn on at or near 0 V. When the turn-on voltage of the MIOS TFD can be shifted from 0 V, various types of devices can be fabricated by simple thin-film processes, such as Zener diodes that maintain a constant voltage even during sudden current changes, as well as transient-voltage-suppression (TVS) diodes that protect circuits from static electricity. The design of the electrostatic discharge (ESD) protection circuit can also be simplified by using a MIOS TFD with a controlled turn-on voltage.

In this work, we demonstrate the MIOS TFDs that can shift the turn-on voltage through its use of a combination of several types of metal and oxide

semiconductors and attempt to verify a new hypothesis based on data newly added to the previous research.[17] When a new metal electrode is deposited on the oxide semiconductor of the MIOS TFD to form a Schottky barrier, electrons can pass through the barrier only when a certain voltage threshold is met or exceeded. As a result, the value of the turn-on voltage of the device becomes positive. Electrons that have passed through the Schottky barrier accumulate in the oxide semiconductor region in contact with the insulator and then flow along the trap or defect states of the insulator to reach the opposite metal. The electrical characteristics of the electrons are analyzed through the vertical current-voltage (I-V) relationship. The contact properties of metal and oxide semiconductors are investigated by the transmission-line method (TLM), time-of-flight secondary ion mass spectrometry (ToF-SIMS), and high-resolution transmission electron microscopy (HRTEM). According to these results, it is expected that extended study focusing the control of the turn-on voltage of the diodes will increase the applicability of MIOS TFDs to various next-generation electronic devices.

3.2 Experimental methods

3.2.1 Preparation of the insulator layer

The SiO_2 layer used as the insulator was deposited up to 200 nm using a thermal

evaporation system (DAEKI HI-TECK) and plasma-enhanced chemical vapor deposition (PECVD, Oxford PlasmaPro System100).

3.2.2 Preparation of the oxide semiconductor layer

Indium gallium zinc oxide (a-IGZO, In:Ga:Zn:O=1:1:1:4 at%, 99.99%) and zinc oxide (ZnO, 99.99%) layers were prepared on SiO_2 layer by a radio frequency (RF) sputtering system. Each oxide semiconductor was deposited to a thickness of 40 nm using a shadow mask with a side length of 1.5 cm. A shadow mask is to prevent unwanted contact between the oxide semiconductor layer and the bottom electrode. The oxide semiconductor's oxygen composition ratio and post-annealing conditions were fixed so that the diode can be turned on near 0 V. All post-annealing was conducted under atmospheric pressure using rapid thermal annealing (RTA). A-IGZO was heat-treated at 425℃ for 90 s, and ZnO was heat-treated at 350℃ for 60 s. The spin coating process was conducted for indium zinc oxide (IZO, 0.2 mol $I_{0.7}Z_{0.3}O$) layer. A precursor was made by dissolving indium hydrate ($In(NO_3)_3 \times H_2O$, 99.999%, Aldrich) 0.84 g and zinc nitrate dihydrate ($Zn(NO_3)_2 \times H_2O$, 99.999%, Aldrich) 0.36 g in 10 ml of 2-methoxyethanol.[17] After the spin coating process, the IZO was heated for 1 h on a hot plate at 350℃.

$I_{0.5}Z_{0.5}O$ and $I_{0.3}Z_{0.7}O$ were prepared by dissolving in 2-methoxyethanol to verify the effect of the difference in indium content on the electrical characteristics of the diode

3.2.3 Deposition of the electrodes

A highly boron-doped p^{++} Si wafer was diced (2.54 cm^2) and used as a bottom electrode of the diode. The top electrodes were formed by evaporating the metal pellet using a thermal evaporation system. Metal pellets were aluminum (Al, 99.99%), silver (Ag, 99.99%), titanium (Ti, 99.99%), and gold (Au, 99.99%). The top metal electrode diameter was 500 μm, and it was deposited in a circular shape using a shadow mask.

3.2.4 TLM measurement

The transmission line method (TLM) was applied to measure contact resistance with each top metal electrode and oxide semiconductor thin film. Highly boron-doped p^{++} Si was used as the bottom electrode, and SiO_2 was used as the insulator. A-IGZO and ZnO were deposited under the same conditions as the diode

fabrication, and TLM shadow mask was used for pattern formation. Al and Ag top electrodes were also used with a TLM shadow mask and deposited with a thickness of 50 nm. The TLM electrode shadow mask's electrode spacing is 30, 50, 70, and 90 μm.

3.2.6 Characterizations

The electrical properties of all devices were measured using an Agilent 4155B. Chemical analysis of the device was performed using a time of flight secondary ion mass spectrometer (TOF-SIMS, IONTOF). For cross-sectional analysis of the device, focused ion beam (FIB, Nova Nanolab) and high-resolution transmission electron microscopy (HR-TEM, FC-TM20) were used.

3.3 Turn-on voltage shift of MIOSM TFD

A device with bottom electrode-insulator-oxide semiconductor-top metal (MIOSM) structure was fabricated by adding a metal layer to control the injection of electrons into the oxide semiconductor layer of the MIOS TFD. A p^{++} Si substrate was used as the bottom electrode, and a charge transfer layer (CTL) of

200 nm of SiO_2 was thermally grown. An electron injection layer (EIL) of 40 nm of a-IGZO was deposited by RF sputtering. The top electrodes were deposited with 50 nm of Al or Ag using a thermal evaporator. The reported work function of Al is 4.06 to 4.26 eV and that of Ag is 4.26 to 4.74 eV.[18] The top electrode was fixed at 0 V and the bottom electrode was swept from -24 V to 24 V to verify the output current characteristics (Figure 3.1(a)). When -24 V was applied to the top electrode, the current was 8.92×10^{-11} A for Al and 7.31×10^{-11} A for Ag. On the other hand, the current of Al at 24 V was 7.71×10^{-5} and that of Ag was 2.28×10^{-6}. Particularly noteworthy is that the turn-on voltage of a diode with Ag is 12.8 V compared to 0 V for Al (Figure 3.1(b)). Ti, having a work function of 4.33 eV,[15] was deposited as a first contact electrode of a-IGZO to a thickness of 20 nm, after which Ag was deposited to a thickness of 50 nm as a second layer. The diode then turned on at 0 V, similarly to Al (Figure 3.2(a)). It is difficult to explain the turn-on voltage difference due to the effect of the Schottky barrier formed by the contact between the a-IGZO with electron affinity of 4.16 eV and each of three types of top metal with similar work functions (Figure 3.2(b)).[19]

The Schottky barrier formed by the contact between the metal and semiconductor follows the equation $\Phi_B=\Phi_M-\chi$, as is well known.[20] Here, Φ_B is

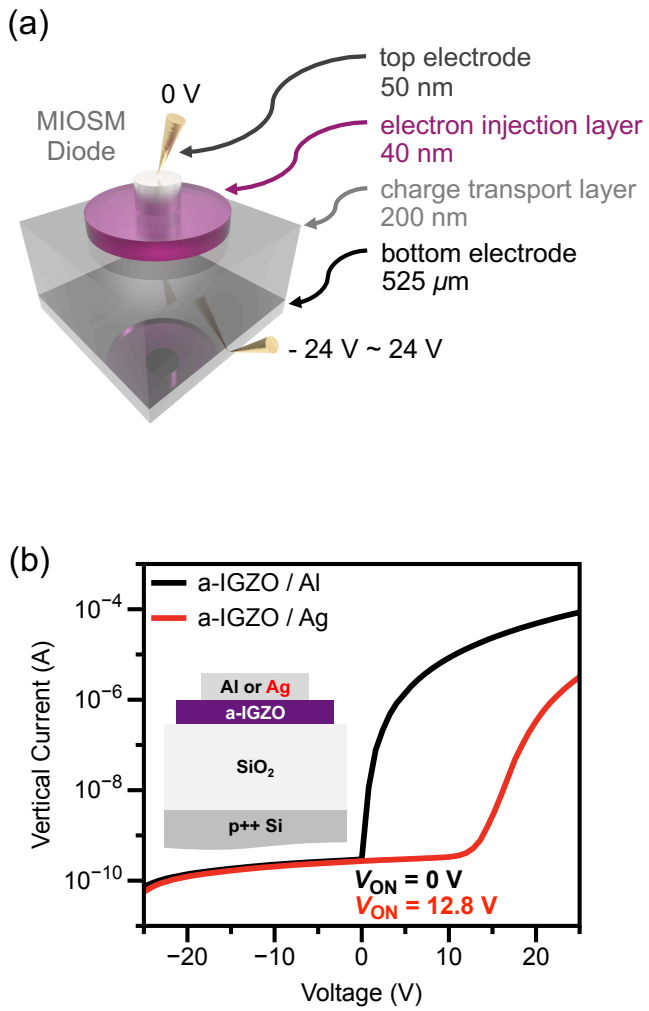

Figure 3.1. (a) Schematic representation of the metal-insulator-oxide semiconductor-metal (MIOSM) device composed of sputtered electron injection layer (EIL), thermally grown electron transport layer (ETL) and electrodes. (b) Vertical current-voltage plots for the devices measured at room temperature; turn-on voltage variation depending on the Al and Ag top metal electrodes.

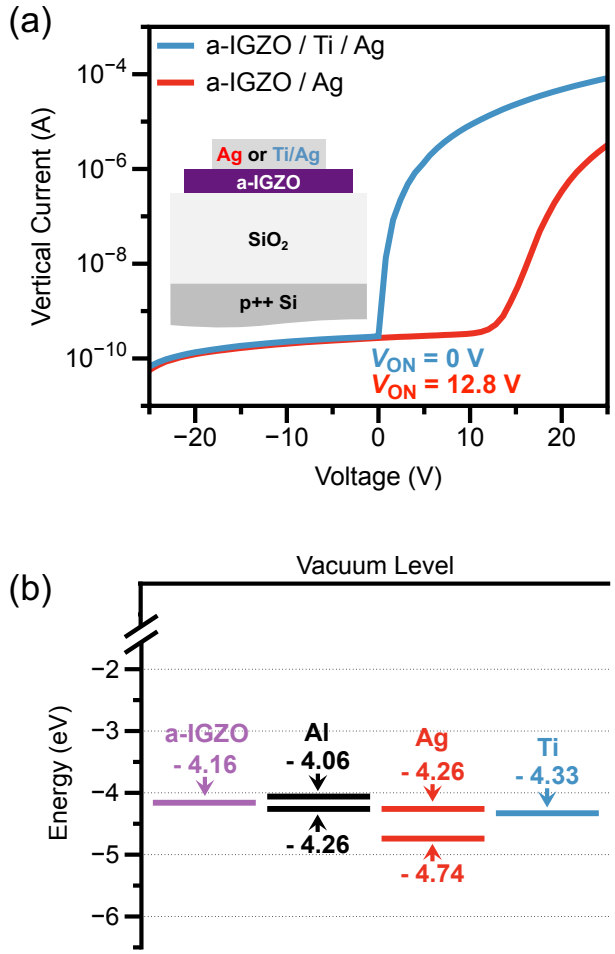

Figure 3.2. (a) Vertical current-voltage plots for the devices measured at room temperature; turn-on voltage variation depending on the Ag and Ti/Ag top metal electrodes. (b) Schematic energy level diagram for the materials used in the MIOSM diodes.

the Schottky barrier height, Φ_M is the work function of the metal, and χ is the electron affinity of the oxide semiconductor. In each case, Φ_B is -0.1 to 0.1 eV for a-IGZO/Al, -0.1 to 0.58 eV for a-IGZO/Ag, and 0.17 eV for a-IGZO/Ti. Furthermore, considering that the TFDs of the a-IGZO/Al and a-IGZO/Ti/Ag contacts turn on at 0 V, ohmic contact characteristics are shown between the two layers, though this is not the case for the Schottky contact. Considering that the TFDs of the a-IGZO/Al and a-IGZO/Ti/Ag turn on at 0 V, the contact of the oxide semiconductor and the metal is ohmic rather than the Schottky type. Moreover, it is unlikely that the Schottky barrier alone shifts the turn-on voltage to 12.8 V, even if Φ_B of a-IGZO/Ag is at the highest reported value of 0.58 eV. Au, having a work function of 5.10 to 5.47 eV,[14] was deposited as a top electrode of a-IGZO TFD to a thickness of 50 nm to compare with the a-IGZO/Ag case. As a result, the turn-on voltage of TFD of a-IGZO/Au was measured at 8.4 V (Figure 3.3(a) and (b)). The work function of Au is 0.84 to 1.41 eV higher than Al. In addition, the Schottky barrier of a-IGZO/Au is 0.94 to 1.31 eV, which is larger than -0.1 to 0.58 eV of a-IGZO/Ag. Therefore, the TFD of a-IGZO/Ag should be less than 8.4 V by calculation. These results suggest that the enhancement of the Schottky contact property plays a key role due to the change in the interface characteristics of a-IGZO/Ag.

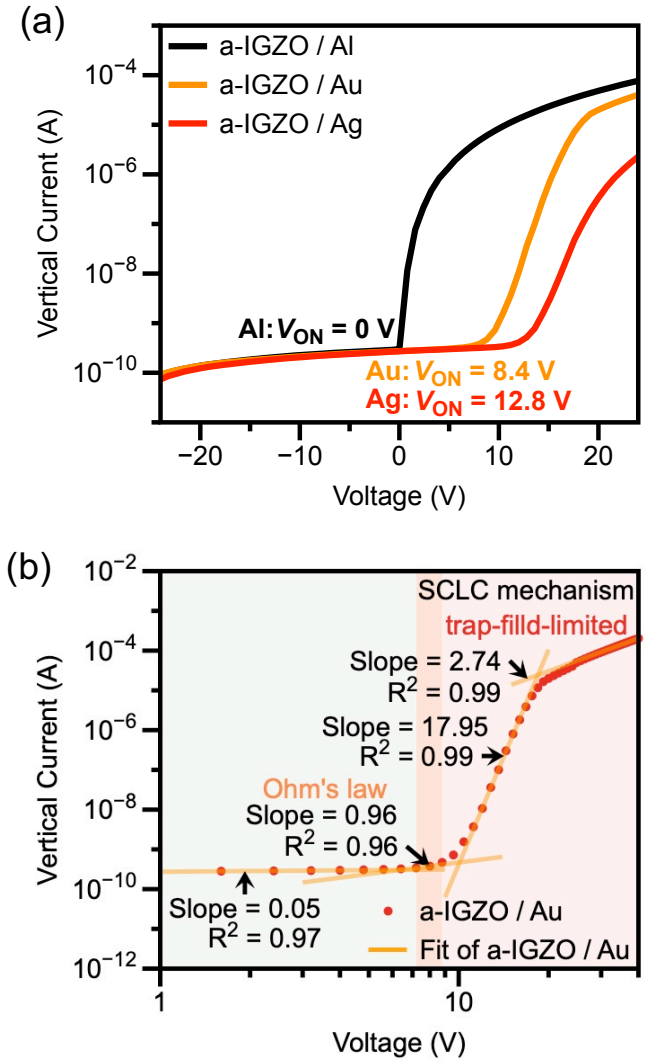

Figure 3.3. Vertical current-voltage (I-V) plots of the a-IGZO-based thin-film diodes (TFDs) measured at room temperature; (a) turn-on voltage variation depending on the top metal electrodes such as Al (0 V), Ag (12.8 V), and Au (8.4 V). (b) electrical characteristics of the TFD with Au electrode.

3.4 Effect of Schottky barrier between oxide semiconductor and electrode

In order to confirm that the increase of the Schottky barrier occurred due to the change of the interface characteristics of a-IGZO/Ag, the contact resistance (R_C) of the metal-semiconductor (MS) was tested by the transmission-line method (TLM).[17,20,21] The R_C value of a-IGZO/Al was 987.7 Ω (Figure 3.4(a)), but the value of a-IGZO/Ag changed from 5807 to 3372 Ω as the voltage was changed from 15 to 20 V, nearly three to five times higher than that of a-IGZO/Al (Figure 3.4(b)). The R_C value of a-IGZO/Ag depends on the change in the voltage, and a-IGZO/Al is independent, meaning that the effect of R_C on the total resistance (R_T) is more significant for a-IGZO/Ag.

When the ratios of R_C to R_T for each of the devices are compared, a-IGZO/Ag is 24.4%, and a-IGZO/Al is 3.3% at a voltage of 16 V and channel length of 90 μm (Figure 3.4(c)). This confirms that electrons passing through the interface of a-IGZO/Ag are significantly affected by R_C. The shorter the channel length is, the lower the sheet resistance becomes, causing the ratio of R_C to R_T to increase. As a result, it was confirmed that when the upper metal was thermally evaporated on a-IGZO deposited by sputtering, the R_C value of a-IGZO/Ag increases more than that of a-IGZO/Al and the Schottky contact becomes noticeable.

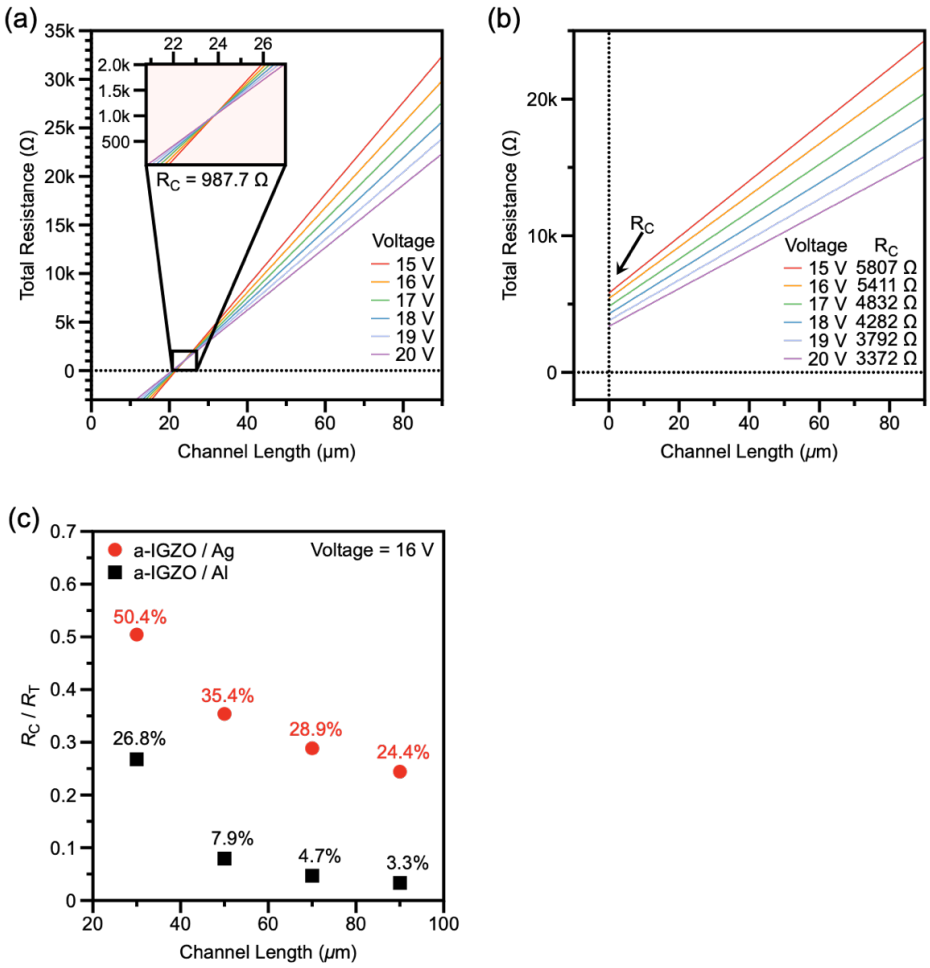

Figure 3.4. Measuring the contact resistance (R_C) of a-IGZO/Al and a-IGZO/Ag via TLM. (a) Total resistance (R_T) of a-IGZO/Al as a function of channel length (L). Inset: R_C between a-IGZO/Al. (b) R_T and R_C of a-IGZO/Ag. (c) R_C/R_T for a-IGZO/Al and a-IGZO/Ag.

3.5 Reversely contacted Ag/AgO_X Schottky diode on MIOS structure

The device was cut vertically using a focused ion beam (FIB), and the cross-section was observed by high-resolution transmission electron microscopy (HRTEM) to check what changes occurred at the oxide semiconductor/metal interface. As a result, a nonspecific layer of 4 to 5 nm was found at the interface of a-IGZO/Ag (Figures 3.5(a) and (b)). An analysis of this layer with time-of-flight secondary ion mass spectrometry (ToF-SIMS) confirmed the formation of a silver oxide (AgO_X) and a-IGZO mixed layer on the a-IGZO surface (Figure 3.6). However, a HRTEM analysis of the a-IGZO/Al contact interface showed no significant interfacial changes between a-IGZO and Al (Figures 3.7(a) and (b)).

To the best of our knowledge, there has been no report of a mixed layer of a-IGZO and AgO_X which forms on the a-IGZO surface when Ag is thermally evaporated on a-IGZO sputtered at room temperature. However, one study reports that when Ag is deposited by means of electron beam evaporation, a region of high resistivity forms.[23] In such as case, AgO_X can form a high-resistivity region in the interlayer of a-IGZO/Ag by oxygen supplied from a-IGZO. The resistivity of AgO_X has been reported to be approximately 10^1 to 10^8 Ω·m, which is 7 to 14 orders higher than the approximate value of 10^{-6} Ω·m for

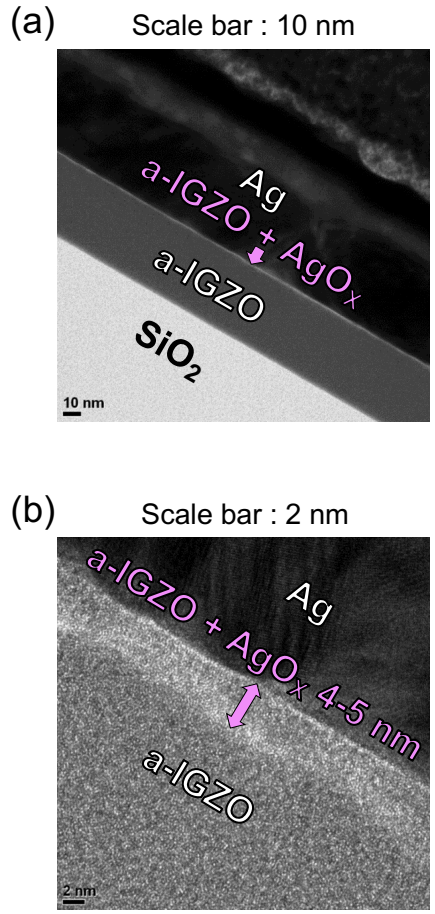

Figure 3.5. Cross-sectional HRTEM images of the interface between the top metal electrode and a-IGZO layer. (a) Vertical structure of MIOS TFD with Ag top electrode, (b) interface between sputtered a-IGZO and thermally evaporated Ag.

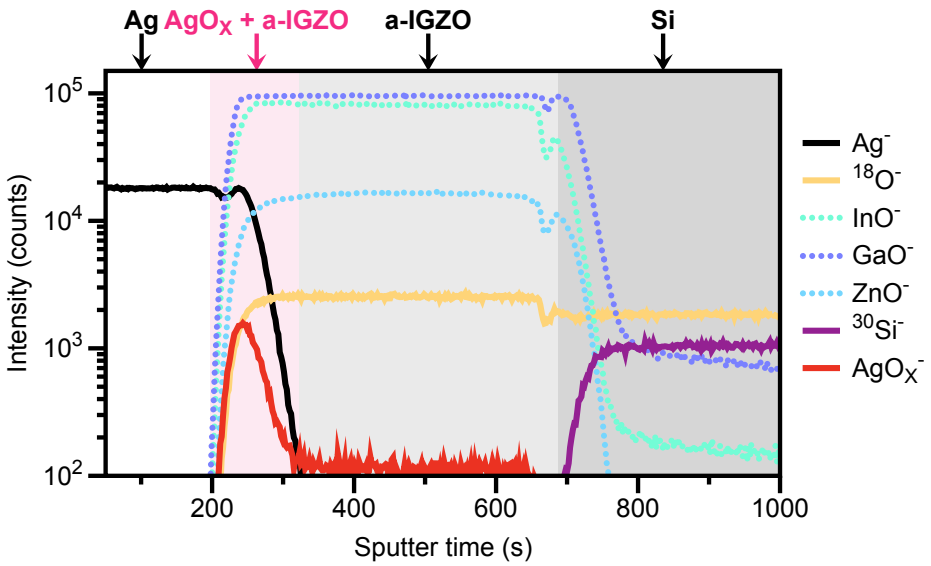

Figure 3.6. TOF-SIMS depth profile analysis of the MIOS TFD with Ag top electrode.

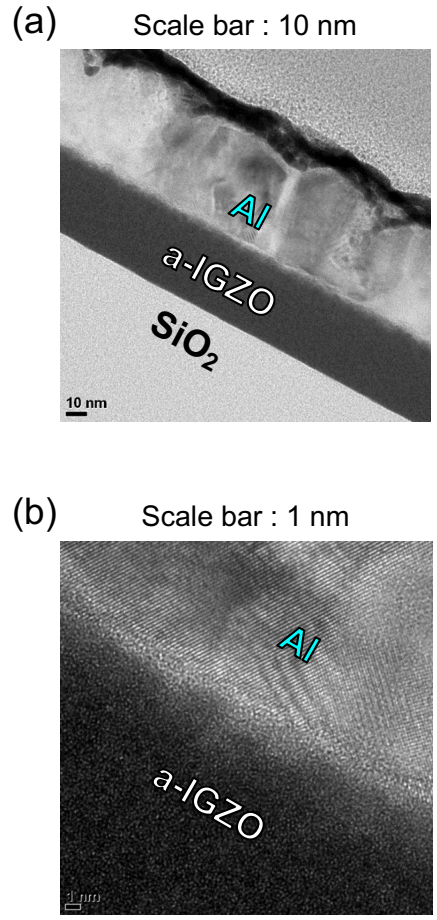

Figure 3.7. Cross-sectional HRTEM images of the interface between the top metal electrode and a-IGZO layer. (a) Vertical structure of MIOS TFD with Al top electrode, and (b) interface between sputtered a-IGZO and thermally evaporated Al.

Ag.[24] Therefore, the measured data indicate that the a-IGZO + AgO_X layer formed in the interlayer of the a-IGZO/Ag contact increased R_C and heightened the Schottky barrier. That is, the high-resistivity AgO_X was mixed with the a-IGZO to form a new type of oxide semiconductor layer of a-IGZO + AgO_X, and this layer is considered to make the characteristics of the Schottky contact between the top metal and the semiconductor more prominent.

Therefore, these results suggest a new structure of a MIOSOSM diode in which an additional Schottky diode of an oxide semiconductor-metal (OSM) contact is added to the oxide semiconductor layer in the MIOS diode to rectify the vertical charge flow, as reported previously. Considering that a Schottky contact is added to the structure of the MIOS diode, it is possible to explain the shift of the turn-on voltage caused by the deposition of Ag on the top electrode, as shown in Figure 1b; the rectifying direction of the Schottky diode formed in the interface is opposite to the rectifying direction of the MIOS diode.

3.6 Charge carrier transport mechanism in turn-on voltage shifted MIOSM TFD

For the case in which the top electrode of the MIOSM (p^{++} Si 525 μm/SiO_2 200 nm/a-IGZO 40 nm/Al 50 nm) or MIOSOSM (p^{++} Si 525 μm/SiO_2 200 nm/a-

IGZO 35-36 nm/a-IGZO + AgO_X 4-5 nm/Ag 50 nm) diode is grounded and the voltage at the bottom electrode is in the range -20 V≤V_{in}≤20 V, this can explain the difference in the mechanism of the electron flow between the bottom and top metals (Figure 3.8).

In the MIOSM structure in which a-IGZO/Al forms an ohmic contact, the electrons supplied to Al are injected into the conduction band of a-IGZO and accumulate in the region of a-IGZO in contact with SiO_2 when V_{in}=20 V (Figure 3.8(a)). The accumulated electrons are injected into a 200-nm-thick SiO_2 insulator and flow to the bottom electrode in the vertical direction of the device according to Child's law of the space-charge-limited conduction (SCLC) mechanism, which is a type of bulk-limited conduction mechanism (Figure 3.9). Conversely, when V_{in}=-20 V, electrons are depleted in the a-IGZO region in contact with SiO_2 such that the electrons supplied from the bottom electrode do not easily reach the top electrode (Figure 3.8(b)).

On the other hand, the diode was not turned on at V_{in}=0 V in the MIOSOSM structure (Figures 3.1(b) and 3.2(a)). Because the voltage range of V_{in}=0-12.8 V is a turn-off region with a reverse bias for the Schottky diode with the a-IGZO + AgO_X/Ag structure, electrons delivered from the top electrode are blocked from crossing the Schottky barrier (Figure 3.10(a)). Most of the electrons that cross the

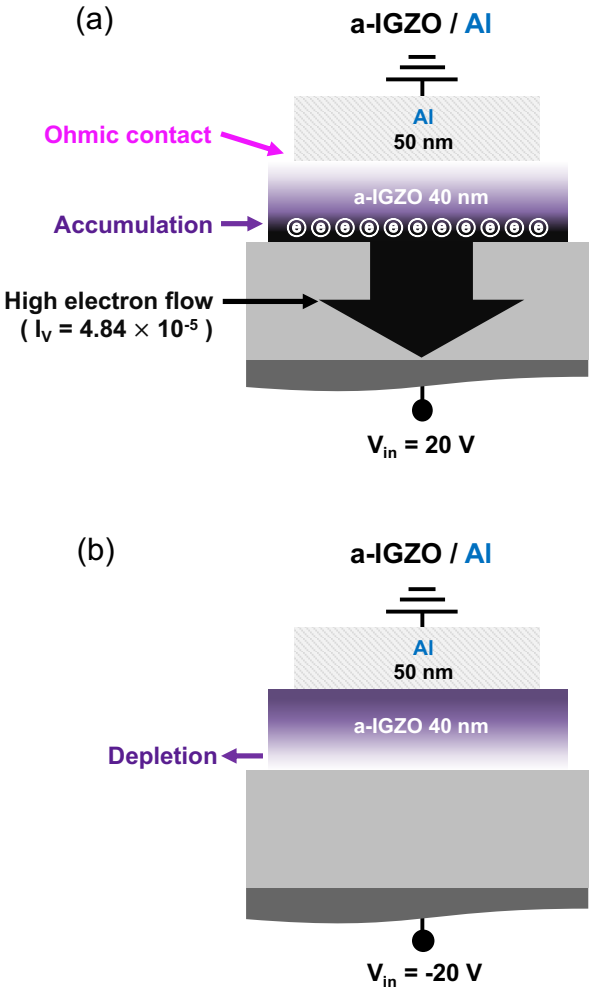

Figure 3.8. Schematic representation of a-IGZO/Al-based TFD (a) in the on-state and (b) off-state.

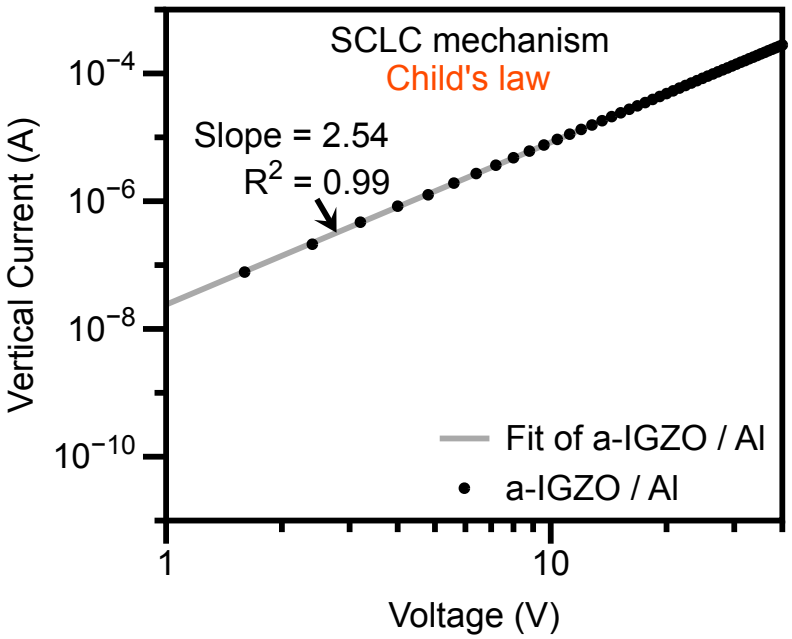

Figure 3.9. I-V relationship of the TFDs on a logarithmic scale with a-IGZO/Al.

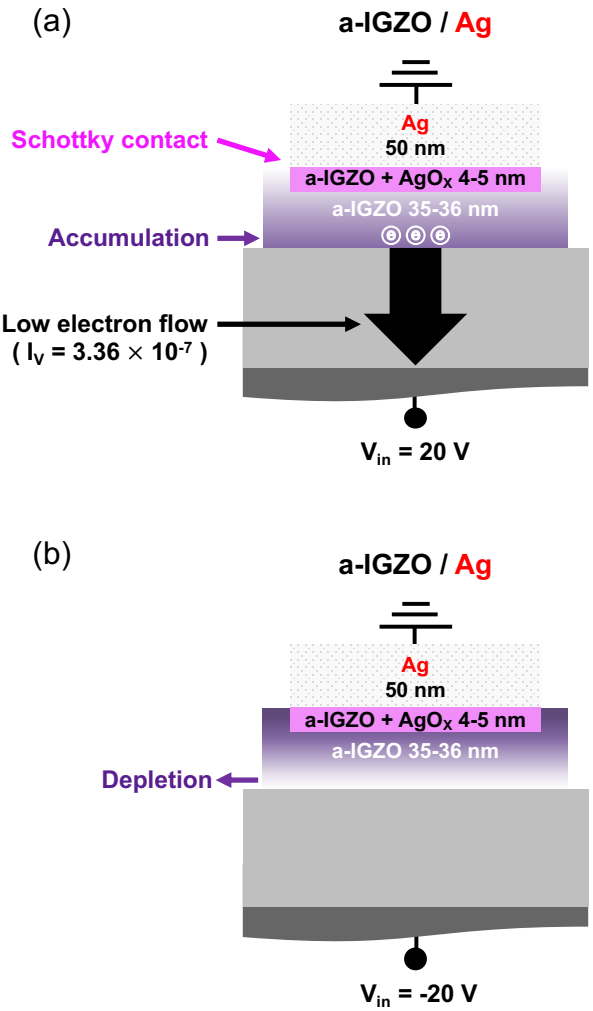

Figure 3.10. Schematic representation of a-IGZO + AgO_X/Ag-based TFD (a) in the on-state and (b) off-state.

Schottky barrier are due to thermionic emission (TE) in this case (Figure 3.11(a) and (b)). As the voltage applied to the bottom electrode exceeds V_{in}=12.8 V, the electrons transferred from the top electrode start tunneling to the Schottky barrier and begin to move to the semiconductor layer. The electrons passing through the a-IGZO + AgO_X/Ag layer migrate along the conduction band of a-IGZO and then accumulate in the a-IGZO region in contact with SiO_2. Even if 20 V is applied to the bottom electrode, the electrons accumulated at the interface of SiO_2/a-IGZO are much smaller than the ohmic contact of a-IGZO/Al. Therefore, the current flowing through the SiO_2 layer is relatively low at the same voltage and the turn-on voltage becomes positive. As the Schottky characteristic due to the a-IGZO + AgO_X/Ag layer is dominant, the turn-on voltage of the TFD shifts. When voltage is applied to the bottom electrode in the range of -20 V≤V_{in}≤0 V, the a-IGZO region in contact with SiO_2 enters a depletion state (Figure 3.10(b)). Because the electrons supplied from the bottom electrode cannot go beyond the depletion region in the a-IGZO, the diode maintains the turn-off state regardless of the presence of the AgO_X layer.

The results of the I-V curve of the TFD that turns on at 0 V when Ti/Ag is thermally deposited can be explained based on the results presented thus far (Figure 3.2(a)). Ti acts as a buffer layer to prevent contact between Ag and

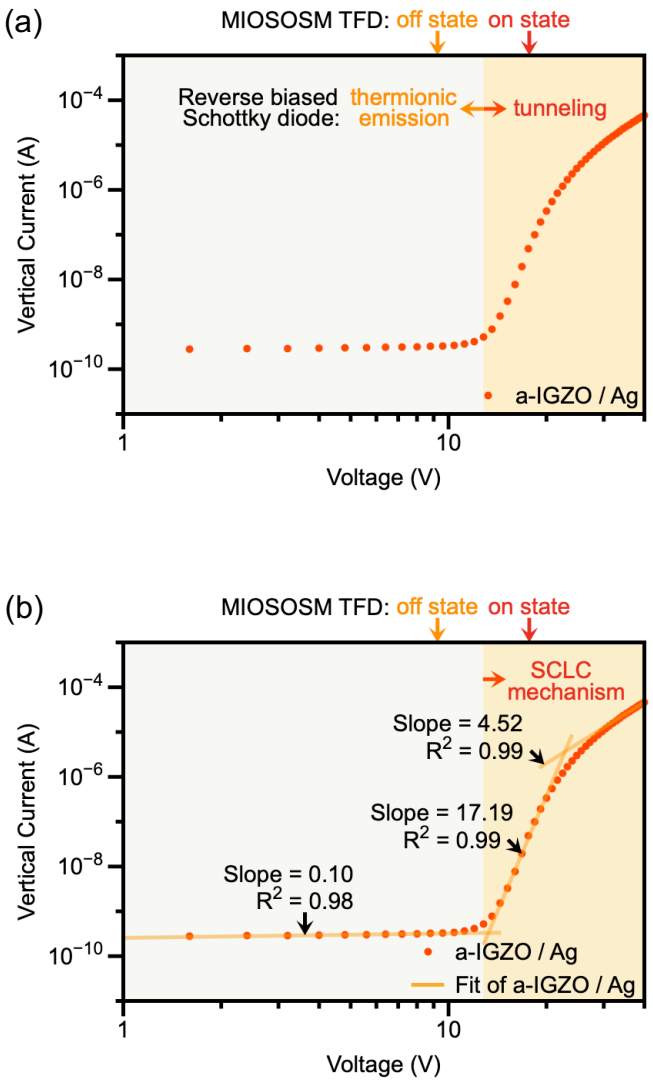

Figure 3.11. I-V relationship of the TFD on a logarithmic scale with (a) a-IGZO + AgO_X/Ag and (b) analysis of charge transfer characteristics according to the on-off state of the TFD.

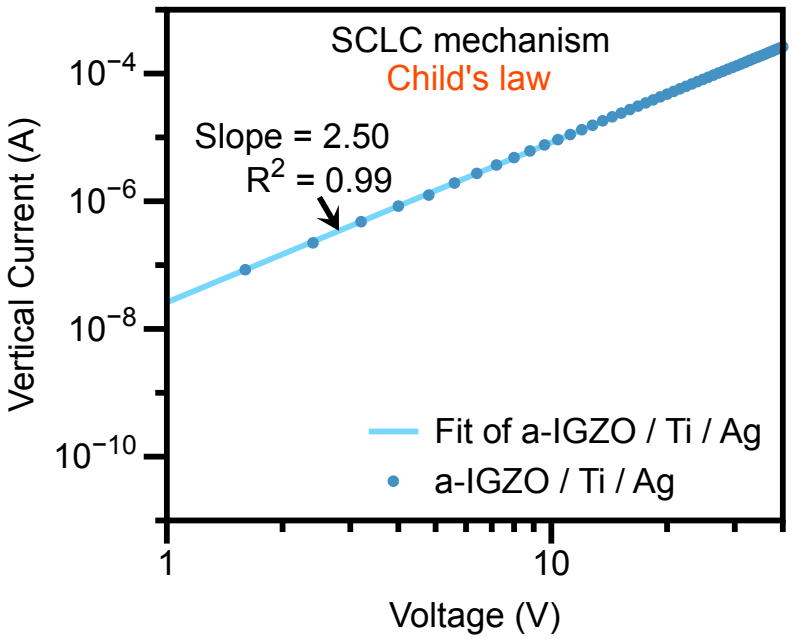

Figure 3.12. I-V relationship of the TFDs on a logarithmic scale with a-IGZO/Ti/Ag. Schematic representation of a-IGZO + AgO_X/Ag-based TFD.

a-IGZO and accordingly to prevent the formation of an a-IGZO + AgO_X layer. Moreover, the contact of Ti and a-IGZO shows ohmic characteristics, similar to the Al and a-IGZO contact, and free electrons can move easily between Ti and Ag. Therefore, when positive voltage is applied to the bottom electrode, electrons move to a-IGZO, which shows ohmic contact characteristics. The electrons then flow along the trap or defect states of SiO_2 and eventually reach p^{++} Si. The characteristics of the current follow Child's law of the SCLC mechanism, as in the case of a-IGZO/Al (Figure 3.12). In contrast, when negative voltage is applied to the bottom electrode, the a-IGZO region in contact with SiO_2 is depleted, which makes it difficult to pass electrons between the electrodes. These results suggest that the turn-on voltage of the MIOS TFD can easily be shifted by adding a Schottky diode in the reverse direction on the oxide semiconductor.

3.7 Turn-on voltage shift of ZnO-based MIOSM TFD

On the other hand, MIOS TFDs were fabricated with different oxide semiconductors to investigate the cause of the formation of the a-IGZO + AgO_X layer when Ag is deposited on sputtered a-IGZO by thermal evaporation. A-IGZO was replaced by sputtered polycrystalline ZnO and the electrical properties of the TFDs were measured. Given that the electron affinity of ZnO is 4.35 eV,[25] the

Schottky barrier height of ZnO/Al is -0.2 to 0.09 eV and that of ZnO/Ag is 0.09 to 0.39 eV. Therefore, ZnO/Ag can form a Schottky contact, and ZnO/Al can create an ohmic contact or a relatively low Schottky barrier. The I-V relationship of the TFDs showed that the turn-on voltage shift of ZnO/Ag was 4.0 V while that of ZnO/Al was -0.8 V (Figure 3.13). These results suggest that the Schottky barrier due to ZnO/Ag causes more resistance than ZnO/Al when the electrons transferred to the top metal electrode of the TFD move to the bottom electrode. It could be confirmed that the R_C value of ZnO/Al is 512.6 Ω, approximately three to six times lower than that of ZnO/Ag (Figures 3.14(a) and (b)). Additionally, the R_C value of ZnO/Ag is dependent on the voltage such that the R_T is affected more by the R_C as opposed to the independent ZnO/Al ratio.

In order to confirm whether this phenomenon was caused by the formation of a new ZnO + AgO_X/Ag layer, similarly to a-IGZO + AgO_X/Ag or only due to the Schottky barrier of ZnO/Ag, the TFD device was cut with FIB and the cross-section was observed with HRTEM (Figure 3.15(a)). As a result, unlike a-IGZO/Ag, the interface of ZnO/Ag did not show an oxide layer such as ZnO + AgO_X. Therefore, AgO_X does not readily form naturally between sputtered ZnO and thermally deposited Ag, and only the Schottky barrier due to the two materials affects the electron flow in the TFD. ZnO/Al was also examined in the

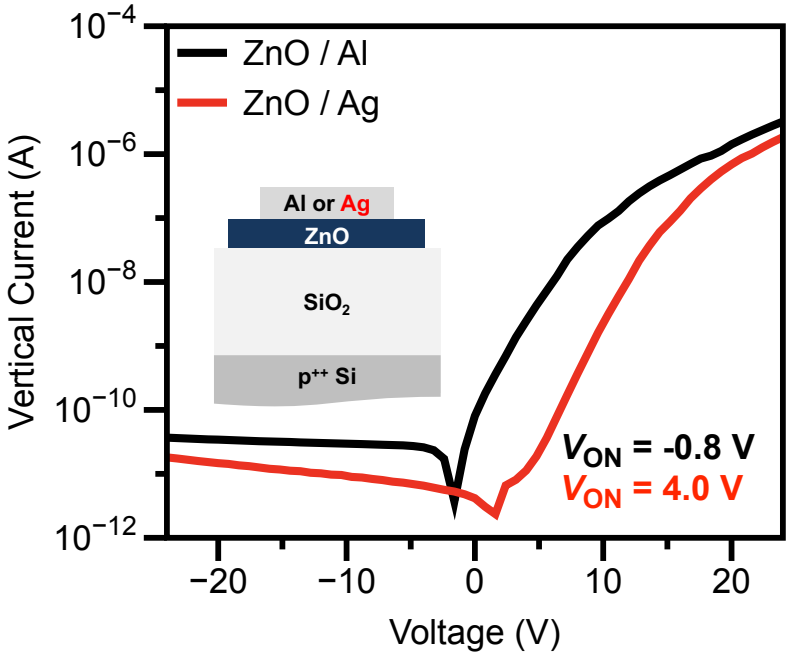

Figure 3.13. Turn-on voltage shift of ZnO-based MIOSM TFD depending on the top metal electrodes.

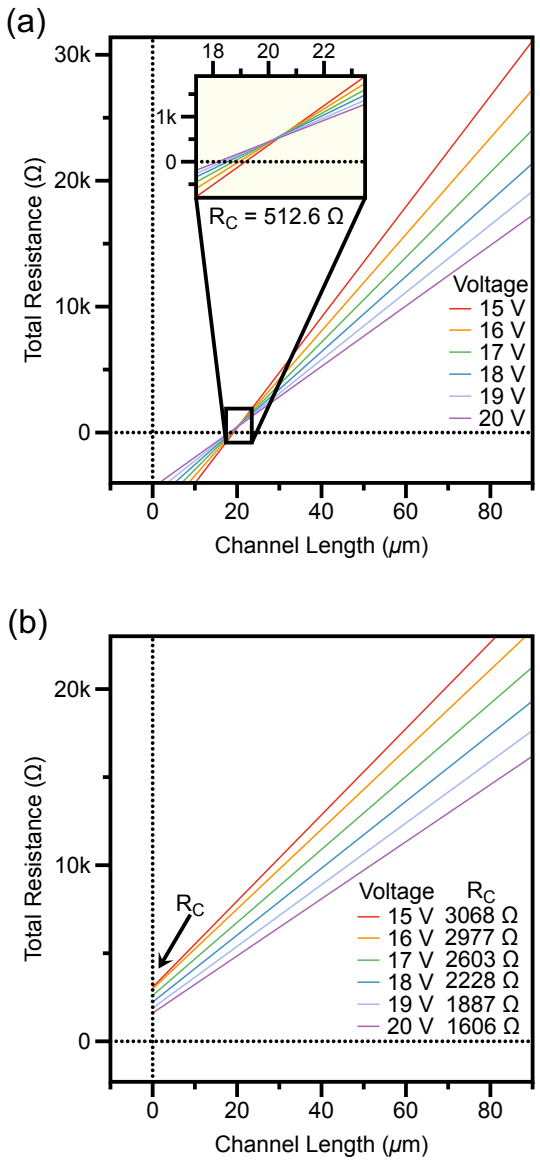

Figure 3.14. Measuring the contact resistance (R_C) of ZnO/Al and ZnO/Ag via transmission-line method (TLM) (a) Total resistance (R_T) of ZnO/Al as a function of channel length (L). Inset: R_C between ZnO/Al. (b) R_T and R_C of ZnO/Ag.

same way, but there was no specific change at the interface (Figure 3.15(b)).

Based on these results, the I-V relationship between ZnO/Al and ZnO/Ag-based TFDs was analyzed on a logarithmic scale to examine the mechanism followed by the electron movement of the two devices. The top electrodes of TFDs were grounded and the bottom electrodes were biased to positive voltages up to 40 V. As a result, ZnO/Al showed the trap-filled-limited current of a SCLC mechanism (Figure 3.16(a)). The diode also showed typical ohmic-like characteristics when considering that the slope obtained from the linear fitting varies from 2.46 to 4.21 at 4.8 V and that the TFD turned on at -0.8 V. Contrarily, in the case of ZnO/Ag, the electron flow of the device along the entire region follows the SCLC mechanism, but it can be divided into two sections with different electrical characteristics (Figure 3.16(b)). Ohm's law dominated the first section up to 4 V with a slope of 1.04 due to the relatively high Schottky barrier formed by ZnO/Ag. In addition, when additional voltage was applied, the slope levels reached 8.66 and 4.72, indicating that the trap-filled-limited current was effective. Thus, at voltages above 4 V, electrons begin to tunnel the Schottky barrier and reach the ZnO layer. The electrons then pass through the trap or defect states of the SiO_2 layer and eventually reach the bottom electrode. Considering the electrical data and results of the HRTEM analysis of the contact surface, ZnO/Ag has a Schottky

(a)

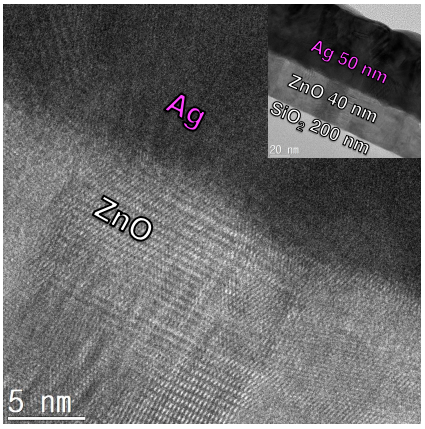

(b)

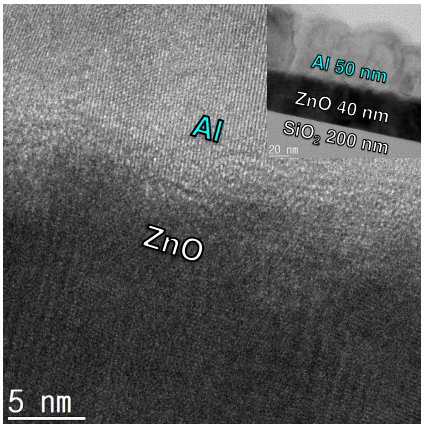

Figure 3.15. Cross-sectional HRTEM images of the interface between (a) sputtered ZnO and thermally evaporated Ag and (b) sputtered ZnO and thermally evaporated Al.

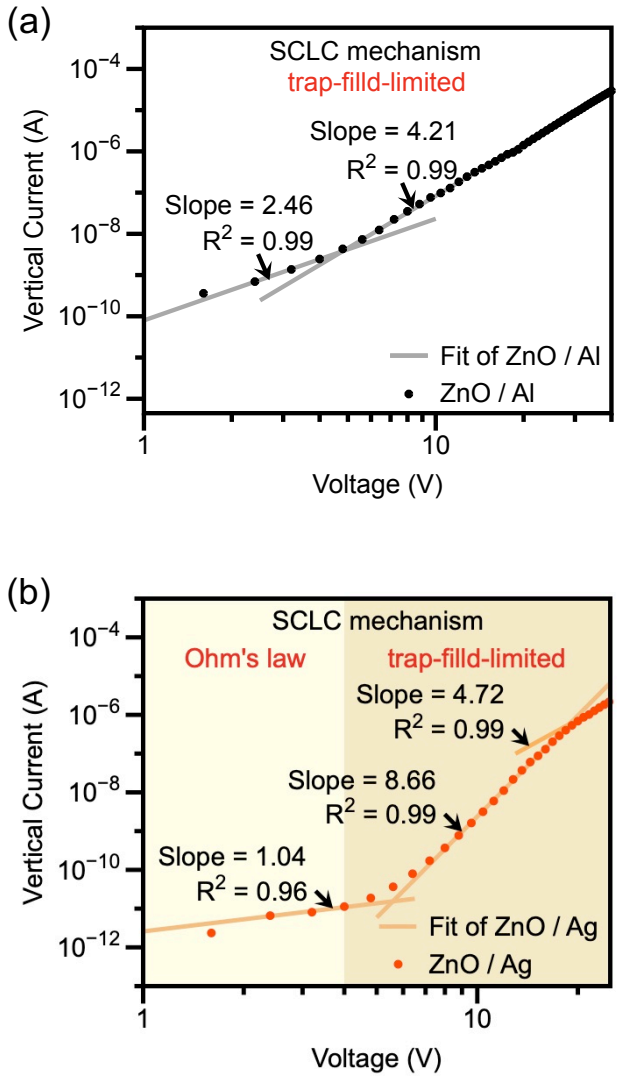

Figure 3.16. I-V relationship of the TFDs on a logarithmic scale with (a) ZnO/Al and (b) ZnO/Ag.

contact, and ZnO/Al shows ohmic-like contact properties. As a result, the TFD of the ZnO/Ag-based MIOSM structure can also shift the turn-on voltage due to the Schottky contact.

3.8 Effect of In-included oxide semiconductor on turn-on voltage shift of MIOSM TFD

In particular, because a ZnO + AgO_X layer did not form at the ZnO/Ag interface, it is suggested that the presence of indium (In) in the oxide semiconductor affects the formation of AgO_X when the Ag is thermally evaporated. In order to test this possibility, a device was prepared using solution-processed IZO with a ratio of In:Zn of 7:3. The turn-on voltages of TFDs were 0.8 V and 0 V for IZO/Al and IZO/Ti/Ag, respectively (Figures 3.17(a) and (b)). However, IZO/Ag did not turn on within 24 V. When the voltage applied was 40 V, on-currents of TFDs using IZO/Al and IZO/Ti/Ag showed the characteristics of an ohmic contact according to Child's law of the SCLC mechanism, whereas IZO/Ag remained in an off-state (Figures 3.18(a), (b), and (c)). These results indicate that the thermal deposition of Ag on IZO containing In also makes the effect of Schottky diode more prevalent, similar to a-IGZO.

In order to check this phenomenon more specifically, IZO/Ag TFDs with In:Zn

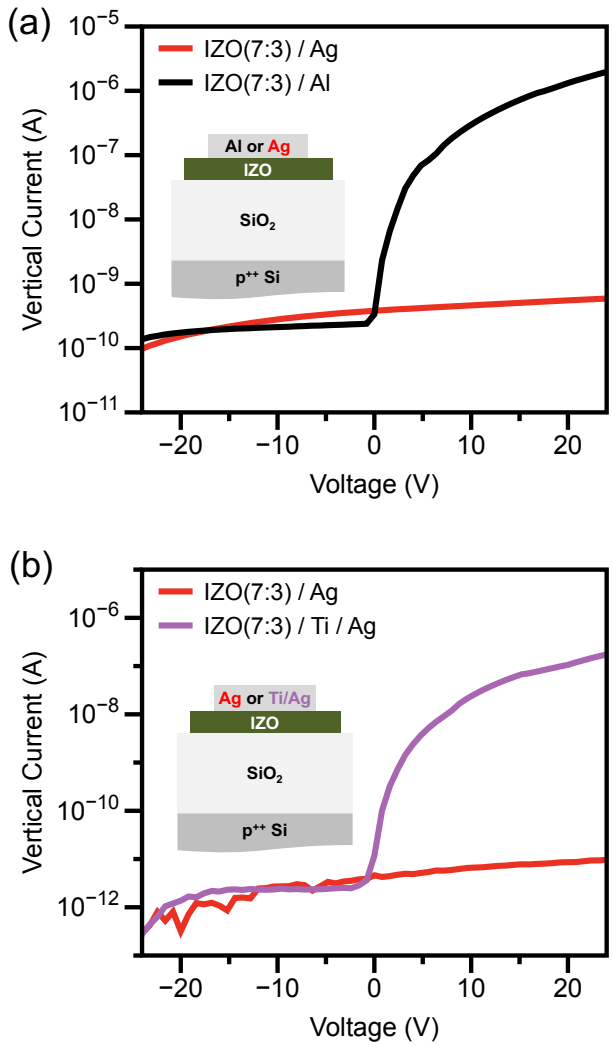

Figure 3.17. Vertical I-V relationships of IZO-based TFDs depending on the top metal electrodes; (a) Al vs Ag and (b) Ag vs Ti/Ag.

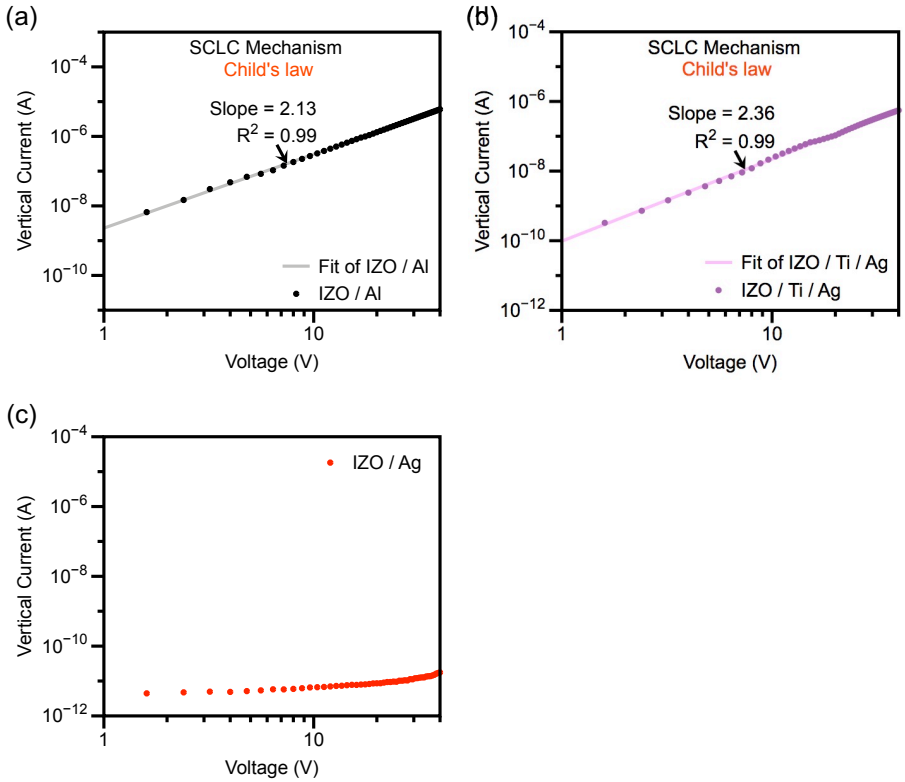

Figure 3.18. I-V relationship of the TFDs on a logarithmic scale with (a) IZO/Al, (b) IZO/Ti/Ag, and (c) IZO/Ag.

ratios of 5:5 and 3:7 were also verified. As the content of In decreases relative to Zn, the IZO/Ag-based TFD showed a higher off-state current (Figure 3.19). Also, the lower the content of In, the lower the voltage converted from off state to SCLC current. The TFD with the lowest ratio of In only turned-on at 13.6 V in the voltage range up to 24 V. These results show the opposite trend to IZO/Al-based TFD. Under positive voltage, when IZO/Ag TFDs were in the off state, the IZO/Al TFDs already reached the on state following the SCLC mechanism (Figure 3.20). Moreover, the higher the relative ratio of indium to zinc, the greater the on-current size at the same voltage due to the increased carrier concentration. The same tendency should be observed for IZO/Ag, but in this case, the higher the relative In ratio was, the smaller the off-current was measured. These results are more explicit evidence of the assumption that the presence or absence of In can change the characteristics of the Schottky contact between the oxide semiconductor and the Ag electrode. Thus, a-IGZO or IZO containing In and the thermally deposited Ag contact are considered to show the characteristics of a Schottky diode that is more dominant than the Schottky contact due to the simple contact between the two materials. However, further study is needed to understand the precise mechanism of how the presence of In dominates the properties of a-IGZO/Ag or IZO/Ag Schottky contacts. An in-depth analysis of

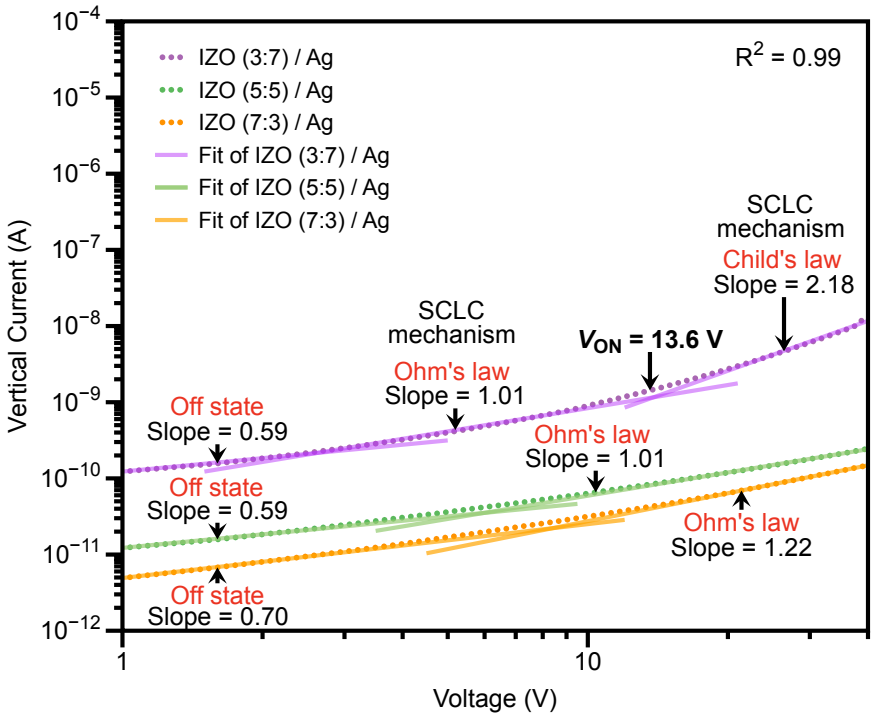

Figure 3.19. Vertical I-V relationships of IZO-based TFDs depending on the different ratio of indium to zinc ($I_{0.3}Z_{0.7}O$, $I_{0.5}Z_{0.5}O$, and $I_{0.7}Z_{0.3}O$) with Ag electrode; Comparison of the amount of thermionic emission in the off state of positive bias depending on the relative content of indium; Comparison of the starting voltage of Ohm's law according to indium content difference under positive bias.

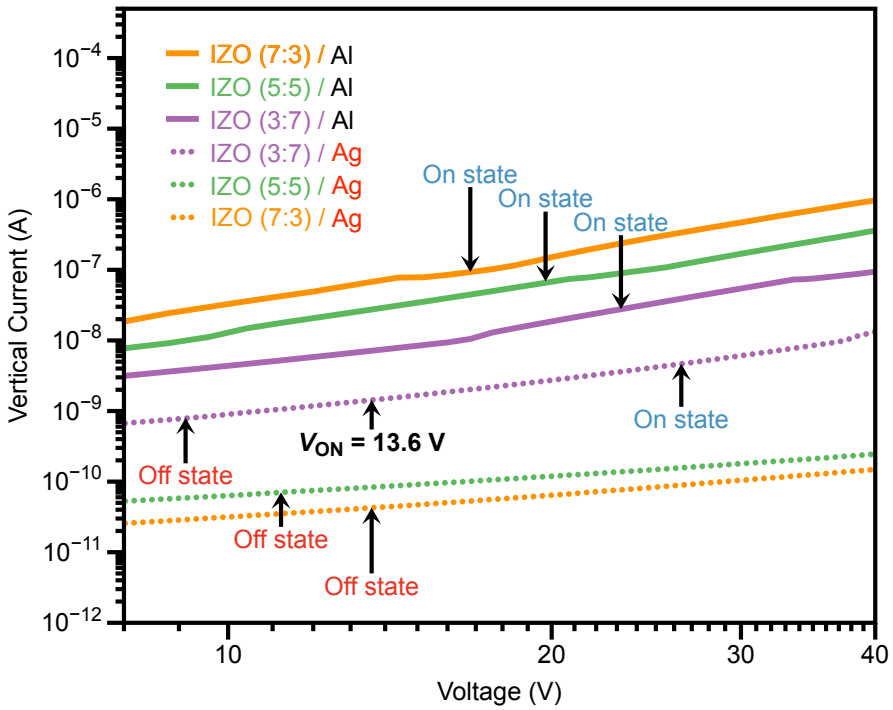

Figure 3.20. Vertical I-V relationships of IZO-based TFDs depending on the different ratio of indium to zinc ($I_{0.3}Z_{0.7}O$, $I_{0.5}Z_{0.5}O$, and $I_{0.7}Z_{0.3}O$) with Al and Ag electrode; On-current comparison of IZO/Al with different indium contents under positive bias (solid line); Comparison of IZO (7:3)/Ag and IZO (5:5)/Ag which maintains the off state and IZO (3:7)/Ag where the turn-on is present.

this phenomenon is expected to enable further fine-tuning of the turn-on voltage shift of MIOS TFDs in the future.

3.9 Conclusion

In conclusion, the turn-on voltage of the MIOS TFD could be controlled by adjusting the characteristics of the Schottky contact of the oxide semiconductor and the top metal. We found that by connecting a metal-oxide semiconductor Schottky diode to a MIOS TFD in the reverse direction, the turn-on voltage of the diode can be changed to a positive voltage. The turn-on voltage was also found to become more positive as the Schottky contact property predominates. A mixed layer of AgO_X and a-IGZO was found to have formed without a post-annealing process when the Ag was deposited onto sputtered a-IGZO via vacuum thermal deposition. When a-IGZO + AgO_X/Ag formed on the top layer of the a-IGZO-based MIOS TFD, the turn-on voltage of the device shifted to 12.8 V due to the enhanced Schottky property. The A-IGZO/Au-based TFD showed a turn-on voltage of 8.4 V shifted due to the reverse Schottky diode formed on the oxide semiconductor. ZnO/Ag showed no noticeable change in the interfacial properties, but the turn-on voltage of TFD shifted to 4.0 V due to the simple Schottky contact between the two materials. The results of a-IGZO and ZnO-based TFD

experiments suggest that the presence or absence of In affects the enhancement of the Schottky contact property by the AgO_X layer when Ag is deposited as an electrode. To confirm the effect of In on the change of the Schottky contact properties, an IZO-based TFD with In:Zn=7:3 was investigated. When Al or Ti/Ag was deposited on the IZO-based MIOS TFD, the device turned on at 0 V. However, when Ag was deposited, the device did not turn on until a voltage of 40 V was applied. As the relative content of indium increased, the on-current of IZO/Al increased as expected, but the off-current was more reduced by the increase of Schottky property of IZO/Ag. These results demonstrate the necessity of a detailed study of how indium in an oxide semiconductor affects the MS interface when depositing Ag on a MIOS TFD as the top electrode. Further studies of this issue will allow for more precise control of the turn-on voltage shift of MIOS TFDs. These results are expected to be useful for those attempting to expand the variety of MIOS TFD specifications and simplify the design of TFD circuits in the future.

3.10 References

(1) Hu, H.; Zhu, C.; Lu, Y. F.; Li, M. F.; Cho, B. J.; Choi, W. K. A High Performance MIM Capacitor Using HfO_2 Dielectrics. *IEEE Electron Device Letters* **2001**, *23* (9), 514–516.

(2) Robertson, J.; Wallace, R. M. High-K Materials and Metal Gates for CMOS Applications. *Materials Science & Engineering R* **2015**, *88*, 1–41.

(3) Wong, H.; Iwai, H. On the Scaling Issues and High-K Replacement of Ultrathin Gate Dielectrics for Nanoscale MOS Transistors. *Microelectronic Engineering* **2006**, *83* (10), 1867–1904.

(4) Cowell, E. W., III; Alimardani, N.; Knutson, C. C.; Conley, J. F., Jr.; Keszler, D. A.; Gibbons, B. J.; Wager, J. F. Advancing MIM Electronics: Amorphous Metal Electrodes. *Adv. Mater.* **2010**, *23* (1), 74–78.

(5) Grover, S.; Moddel, G. Engineering the Current-Voltage Characteristics of Metal-Insulator-Metal Diodes Using Double-Insulator Tunnel Barriers. *Solid State Electronics* **2012**, *67* (1), 94–99.

(6) Urcuyo, R.; Duong, D. L.; Jeong, H. Y.; Burghard, M.; Kern, K. High Performance Graphene-Oxide-Metal Diode Through Bias-Induced Barrier

Height Modulation. *Adv. Electron. Mater.* **2016**, *2* (9), 1600223–1600226.

(7) Chiu, F.-C. A Review on Conduction Mechanisms in Dielectric Films. *Advances in Materials Science and Engineering* **2014**, *2014* (7), 1–18.

(8) Sawa, A. Resistive Switching in Transition Metal Oxides. *Biochemical Pharmacology* **2008**, *11* (6), 28–36.

(9) Esposito, D. V.; Levin, I.; Moffat, T. P.; Talin, A. A. H_2 Evolution at Si-Based Metal-Insulator-Semiconductor Photoelectrodes Enhanced by Inversion Channel Charge Collection and H Spillover. *Nature Materials* **2013**, *12* (6), 562–568.

(10) Ji, L.; Hsu, H.-Y.; Li, X.; Huang, K.; Zhang, Y.; Lee, J. C.; Bard, A. J.; Yu, E. T. Localized Dielectric Breakdown and Antireflection Coating in Metal–Oxide–Semiconductor Photoelectrodes. *Nature Materials* **2016**, *16* (1), 127–131.

(11) Xu, W.; Wang, H.; Ye, L.; Xu, J. The Role of Solution-Processed High-K Gate Dielectrics in Electrical Performance of Oxide Thin-Film Transistors. *J. Mater. Chem. C* **2014**, *2* (27), 5389–5396.

(12) Lampert, M. A. Injection Currents in Insulators. *Proceedings of the IRE* **1962**, *50* (8), 1781–1796.

(13) Choi, M.-J.; Kim, M.-H.; Choi, D.-K. A Transparent Diode with High

Rectifying Ratio Using Amorphous Indium-Gallium-Zinc Oxide/SiN_X coupled Junction. *Applied Physics Letters* **2015**, 107 (5), 053501–053505.

(14) Kim, M.; Choi, S.; Oh, H.; Kim, J.; Choi, D.-K. 76-3: a New Photosensitive Oxide Diode. *SID Symposium Digest of Technical Papers* **2018**, 49 (1), 1021–1023.

(15) Lee, J.; Yoon, K.; Lim, K.-H.; Park, J.-W.; Lee, D.; Cho, N.-K.; Kim, Y. S. Vertical Transport Control of Electrical Charge Carriers in Insulator/Oxide Semiconductor Hetero-Structure. *Scientific Reports* **2018**, *8* (1), 5643-5651.

(16) Kudo, A.; Yanagi, H.; Ueda, K.; Hosono, H.; Kawazoe, H.; Yano, Y. Fabrication of Transparent P–N Heterojunction Thin Film Diodes Based Entirely on Oxide Semiconductors. Applied Physics Letters **1999**, 75 (18), 2851–2853.

(17) J.-W. Park. A Study of Metal Influence on Widening Operating Voltage of Oxide Thin Film Diodes. **2017**.

(18) Leprince-Wang, Y. *Piezoelectric ZnO Nanostructure for Energy Harvesting*, 1st ed; John Wiley & Sons: Hoboken, NJ, **2015**; Chapter 1, pp 5.

(19) Fung, T.-C.; Chuang, C.-S.; Chen, C.; Abe, K.; Cottle, R.; Townsend, M.; Kumomi, H.; Kanicki, J. Two-Dimensional Numerical Simulation of Radio Frequency Sputter Amorphous In–Ga–Zn–O Thin-Film Transistors. *Journal of*

Applied Physics **2009**, *106* (8), 084511–084511.

(20) Sze, S.M.; Ng, K. *Physics of Semiconductor Devices*, 3rd ed; John Wiley & Sons: Hoboken, NJ, 2006; Chapter 3, pp 136.

(21) Rha, S. H.; Jung, J.; Jung, Y.; Chung, Y. J.; Kim, U. K.; Hwang, E. S.; Park, B. K.; Park, T. J.; Choi, J.-H.; Hwang, C. S. Performance Variation According to Device Structure and the Source/Drain Metal Electrode of a-IGZO TFTs. *IEEE Transactions on Electron Devices* **2012**, *59* (12), 3357–3363.

(22) Xu, Y.; Liu, C.; Amegadze, P. S. K.; Park, W.-T.; Long, D. X.; Minari, T.; Balestra, F.; Ghibaudo, G.; Noh, Y.-Y. Significant Roles of Low-Temperature Post-Metallization Annealing in Solution-Processed Oxide Thin-Film Transistors. *Applied Physics Letters* **2014**, *105* (13), 133505–133506.

(23) Ueoka, Y.; Ishikawa, Y.; Bermundo, J. P.; Yamazaki, H.; Urakawa, S.; Osada, Y.; Horita, M.; Uraoka, Y. Effect of Contact Material on Amorphous InGaZnO Thin-Film Transistor Characteristics. *Jpn. J. Appl. Phys.* **2014**, *53* (3S1), 03CC04-1–03CC04-5.

(24) Al-Kuhaili, M. F. Characterization of Thin Films Produced by the Thermal Evaporation of Silver Oxide. *J. Phys. D: Appl. Phys.* **2007**, *40* (9), 2847–2853.

(25) Feng, Z. C. *Handbook of Zinc Oxide and Related Materials: Volume Two,*

Devices and Nano-Engineering, 1st ed; John Wiley & Sons: Boca Raton, Fl, 2012; Chapter 3, pp 91.

Chapter 4 Conclusion

The electrical properties of materials expressed at the oxide interface have been successfully led to the development of new devices such as solar cells and oxide thin-film transistors. However, even though the oxide thin-film diode is a fundamental element of an electronic circuit, it has shown a low rectification ratio of less than 10^3 so far. Oxide thin-film diodes such as P-N junction structure, MIM structure, and MS structure have been reported, but there have been limitations such as low rectification ratio, high off current, and low withstand voltage. Oxide thin-film diodes such as P-N junction structure, MIM structure, and MS structure have been reported, but there have been limitations such as low rectification ratio, high off current, and low withstand voltage. The novel oxide thin-film diode (TFD) has a metal-insulator-oxide semiconductor-metal (MIOSM) structure, and charge carriers are injected or not injected into the trap states inside the insulator according to the electrical state of the oxide semiconductor. The diode shows an excellent rectification ratio over 10^6. MIOSM TFD exhibits high reproducibility using one oxide semiconductor, compared to P-N junction diodes, which inevitably have difficulty controlling electrical properties due to the junction of two oxide semiconductors. In addition, in the case of MIM TFD, it is

challenging to secure uniformity in a large area process because of the thin insulator that relies on quantum tunneling. However, MIOSM TFD can be demonstrated uniformly for the large-area process using conventional semiconductor equipment. Though, despite the excellent electrical properties and convenience of the process, a new oxide thin-film diode has not been manufactured using a p-type oxide semiconductor until now. Also, all MIOSM TFDs reported so far are only turned on near 0 V. These two electrical characteristics are necessary because when MIOSM TFD is applied to a circuit, it can increase the convenience of circuit design and reduce process cost. In this thesis, MIOSM TFD was demonstrated based on a p-type oxide semiconductor, and the result of controlling the turn-on voltage of a new oxide TFD was secured. As a result, it was confirmed for the first time that the advantages of the n-type oxide-based MIOSM TFD, which exceeded the limitations of the conventional oxide thin-film diode, can be achieved by using the p-type NiO_X oxide. The mechanism of rectification characteristics of the device according to hole transportation was also analyzed. Additionally, it was shown that a diode fabricated using a p-type oxide semiconductor could respond to high voltage and low voltage driving. A transparent p-type MIOSM TFD was also demonstrated for the first time. A method of changing the turn-on voltage required to diversify

the specifications of the diode was also presented for the first time. It was necessary to change the diode's turn-on voltage to increase the flexibility and ease of manufacture of the circuit design by expanding the specifications of the n-type oxide-based MIOSM TFD, which exceeded the limitations of the conventional oxide thin-film diode. The turn-on voltage of the MIOSM TFD can be adjusted by stacking the Schottky diode between the oxide semiconductor layer and the upper metal in the opposite direction. It was verified that the turn-on voltage could be easily controlled by enhancing or reducing the Schottky characteristic. This study's significance can be found in that it was the first to propose a method of switching the turn-on voltage of MIOSM TFD. In conclusion, with the reverse idea of making an oxide thin film rectifying device using an insulator known to be unable to flow current, a study was conducted to report a novel oxide TFD based on p-type oxide semiconductors for the first time. We have also secured a method of adjusting the turn-on voltage, changing the operating voltage range, and manufacturing a transparent diode for various applications and expandability of diodes. These research achievements, which further expand the specifications of the MIOSM TFDs fabricated using n-type oxide semiconductors, are expected to play a significant role in the practical application of the novel oxide TFD.

요 약 (국문초록)

금속-절연체-산화물 반도체-금속 접합 구조 산화물 박막 다이오드의 전하 캐리어 이동에 관한 연구

박 준 우
융합과학부 나노융합전공
융합과학기술대학원
서울대학교

스위칭 소자 역할을 하는 산화물 박막 다이오드 (TFD)와 박막 트랜지스터 (TFT)는 차세대 전자 회로의 필수 요소이다. 그러나 성공적인 산업적 응용이 이뤄진 산화물 TFT와 달리 산화물 TFD 관련 개발은 상대적으로 부족한 실정이다. 최근 산화물을 기반으로 기존 산화물 TFD 종류들인 PN 다이오드, 금속-절연체-금속 (metal-insulator-metal, MIM) 다이오드, 쇼트 키 다이오드 등이 보이는 전기적 불안정성, 낮은 작동 전압 범위, 낮은 정류 비율 등을 극복한 새로운 유형의 금속-절연체-산화물 반도체-금속 (Metal-Insulator-Oxide Semiconductor-Metal, MIOSM) 구

조 산화물 TFD가 보고되고 있다. 새로운 MIOSM 구조 기반의 산화물 TFD는 산화물 반도체 표면에서 전하가 주입 될 때 전하 캐리어가 절연체 내부의 트랩 상태를 통해 이동하고, 산화물 반도체 표면이 공핍되면 캐리어가 절연체에 주입되지 않는 원리를 기반으로 작동한다. 이러한 특성을 통해 우수한 전기적 안정성과 높은 정류율을 가진 새로운 개념의 TFD가 개발되고 있다. 한편, 이전에 발표된 모든 MIOSM TFD는 n형 산화물 재료를 기반으로 제작되어 왔다. 전자 회로 구성의 유연성을 높이기 위해서는 p형 산화물 재료를 사용한 MIOSM TFD 개발이 필요한 실정이다. 또한 새로운 TFD의 확장성을 높이기 위해서는 저전압 구동, 고전압 응답, 제너 다이오드와 같은 다양한 유형의 MIOSM TFD가 필요하다. 그뿐만 아니라, MIOSM TFD의 다양한 사양 확보를 통한 산업적 응용을 위해서는 다이오드의 턴온 전압을 전환하는 방법을 찾는 것은 필수적이지만 지금까지 보고된 모든 MIOSM TFD는 0 V 또는 그 근처에서 켜지는 한계를 나타내 왔다. 회로 설계를 단순화하기 위해서는 다양한 전압에서 턴온하는 MIOSM TFD를 제작할 필요가 있다. 따라서 앞서 언급한 한계점들을 극복한, p 형 니켈 산화물 기반 MIOSM TFD와 턴온 전압이 조절 가능한 MIOSM TFD를 제안하는 바이다. 기존의 n형 산화물 기반 MIOSM TFD와는 달리 p형 산화물 기반 다이오드는 절연체 내부의 정공 전도를 기반으로 전류를 정류한다. 니켈 산화물 기반 산화물 박막 다이오드는

10^5 이상의 안정적인 정류 비율을 보여 주며, 작동 전압 범위를 ±8 V에서 ±80 V까지로 좁히거나 넓힐 수 있는 장점이 있다. 또한 인듐 주석 산화물 (ITO)을 전극으로 적용하여, 최초의 투명한 p 형 MIOSM TFD를 시연하였다. 저전압 및 고전압에 대응할 수 있는 새로운 p 형 니켈 산화물 기반 TFD는 n형 MIOSM TFD와 함께 차세대 전자 회로의 기본 구성 요소가 될 것으로 기대된다. 또한 본 연구를 바탕으로 다양한 p 형 산화물 기반 MIOSM TFD가 개발될 것으로 판단된다. 한편, 산화물 반도체에 금속 전극을 추가함으로써 금속 전극과 산화물 반도체 사이의 쇼트키 접촉의 특성 변화에 따라 MIOSM TFD의 턴온 전압을 조절할 수 있었다. 이러한 발견은 MIOSM TFD의 다양성 확대를 가속화하고 MIOSM 다이오드의 산업 응용을 촉진할 것으로 기대된다.

주요어: 박막 다이오드, 금속-절연체-산화물 반도체-금속 구조 박막 다이오드, P타입 니켈 산화물, 쇼트키 다이오드, 투명 박막 다이오드

학 번: 2017-36180